

# Search for narrow six-quark states in the reactions <sup>\*</sup> $\gamma d \rightarrow \pi \gamma NN$

L.V. Fil'kov <sup>†</sup> and V.L. Kashevarov <sup>‡</sup>

Lebedev Physical Institute, Leninsky Prospect 53, Moscow, Russia

## Abstract

We study the reactions  $\gamma d \rightarrow \pi \gamma NN$  with the aim to search for six-quark states, the decay of which into two nucleons is forbidden by the Pauli exclusion principle. Such states predicted by a variety of QCD inspired models and recent evidence from Proton Linear Accelerator of INR (Moscow) strongly suggests the existence of such states with masses 1904, 1926, and 1942 MeV. We propose an experiment at MAMI-B which will provide an unique opportunity to observe such dibaryon states in mass region up to 2000 MeV and determine their masses and quantum numbers.

arXiv:nucl-th/0409009v1 3 Sep 2004

---

<sup>\*</sup>Talk presented at the 5th Crystal Ball Meeting, Mainz, 19-21 March 2004

<sup>†</sup>E-mail: filkov@sci.lebedev.ru

<sup>‡</sup>E-mail: kashev@kph.uni-mainz.de

# 1 Introduction

The possibility of the existence of multi-quark states was predicted by QCD inspired models [1, 2]. These works initiated a lot of experimental searches for six-quark states (dibaryons). Usually one looked for dibaryons in the  $NN$  channel (see for review ref. [3]). Such dibaryons have decay widths from a few up to hundred MeV. Their relative contributions are small enough and the background contribution is big and uncertain as a rule. All this often leads to contradictory results.

In the present work we consider six-quark states, a decay of which into two nucleons is forbidden by the Pauli exclusion principle [4–8]. Such states satisfy the following condition:

$$(-1)^{T+S}P = +1 \quad (1)$$

where  $T$  is the isospin,  $S$  is the internal spin, and  $P$  is the dibaryon parity. In the  $NN$  channel, these six-quark states would correspond to the following forbidden states: even singlets and odd triplets with the isotopic spin  $T = 0$  as well as odd singlets and even triplets with  $T = 1$ . These six-quark states with the masses  $M < 2m_N + m_\pi$  ( $m_N(m_\pi)$  is the nucleon (pion) mass) can mainly decay by emitting a photon. This is a new class of metastable six-quark states with the decay widths  $< 1\text{keV}$ . Such states were called supernarrow dibaryons (SND). The experimental discovery of the SNDs would have important consequences for particle and nuclear physics and astrophysics.

In the framework of the MIT bag model, Mulders et al. [2] calculated the masses of different dibaryons, in particular,  $NN$ -decoupled dibaryons. They predicted dibaryons  $D(T = 0; J^P = 0^-, 1^-, 2^-; M = 2.11 \text{ GeV})$  and  $D(1; 1^-; 2.2 \text{ GeV})$  corresponding to the forbidden states  $^{13}P_J$  and  $^{31}P_1$  in the  $NN$  channel. However, the dibaryon masses obtained exceed the pion production threshold. Therefore, these dibaryons preferentially decay into the  $\pi NN$  channel and their decay widths are large than 1 MeV.

Using the chiral soliton model, Kopeliovich [9] predicted that the masses of  $D(T = 1, J^P = 1^+)$  and  $D(0, 2^+)$  SNDs exceeded the two nucleon mass by 60 and 90 MeV, respectively. These values are lower than the pion production threshold.

In the framework of the canonically quantized biskyrmion model, Krupnovnickas *et al.* [10] obtained an indication on possibility of the existence of one dibaryon with  $J=T=0$  and two dibaryons with  $J=T=1$  with masses smaller than  $2m_N + m_\pi$ .

Unfortunately, all values obtained for the dibaryon masses are model dependent. Therefore, only an experiment could answer the question about the existence of SNDs and determine their masses. In the following, we summarize the experimental attempts to look for such SNDs so far.

In ref. [11–18], the reaction  $pd \rightarrow p + pX_1$  and  $pd \rightarrow p + dX_2$  were studied with the aim of searching for SND. The experiment was carried out at the Proton Linear Accelerator of INR with 305 MeV proton beam using the two-arm mass spectrometer TAMS. As was shown in ref. [14, 15], the nucleons and the deuteron from the decay of SND into  $\gamma NN$  and  $\gamma d$  have to be emitted into a narrow angle cone with respect to the direction of the dibaryon motion. On the other hand, if a dibaryon decays mainly into two nucleons, then the expected angular cone of emitted nucleons must be more than  $50^\circ$ . Therefore, a detection of the scattered proton in coincidence with the proton (or the deuteron) from the decay of the dibaryon at

correlated angles allows the suppression of the contribution of the background processes and increases the relative contribution of a possible SND production.

Several software cuts have been applied to the mass spectra in these works. In particular, the authors limited themselves by the consideration of an interval of the proton energy from the decay of the  $pX_1$  states, which was determined by the kinematics of the SND decay into  $\gamma NN$  channel. Such a cut is very important as it provides a possibility to suppress the contribution from the background reactions and random coincidences essentially.

In the works [16–18],  $\text{CD}_2$  and  $^{12}\text{C}$  were used as targets. The scattered proton was detected in the left arm of the spectrometer TAMS at the angle  $\theta_L = 70^\circ$ . The second charged particle (either  $p$  or  $d$ ) was detected in the right arm by three telescopes located at  $\theta_R = 34^\circ, 36^\circ, \text{ and } 38^\circ$ .

As a result, three narrow peaks in missing mass spectra have been observed (Fig. 1a) at  $M_{pX_1} = 1904 \pm 2, 1926 \pm 2, \text{ and } 1942 \pm 2$  MeV with widths equal to the experimental resolution ( $\sim 5$  MeV) and with numbers of standard deviations (SD) of 6.0, 7.0, and 6.3, respectively. It should be noted that the dibaryon peaks at  $M = 1904$  and  $1926$  MeV had been observed earlier by same authors in ref. [11–15] at somewhat different kinematical conditions. On the other hand, no noticeable signal of the dibaryons has been observed in the missing mass  $M_{dX_2}$  spectra of the reaction  $pd \rightarrow p + dX_2$ . The analysis of the angular distributions of the protons from the decay of  $pX_1$  states and the suppression observed of the SND decay into  $\gamma d$  showed that the peaks found can be explained as a manifestation of the isovector SNDs, the decay of which into two nucleons is forbidden by the Pauli exclusion principle.

An additional information about the nature of the observed states was obtained by studying the missing mass  $M_{X_1}$  spectra of the reaction  $pd \rightarrow p + pX_1$ . If the state found is a dibaryon decaying mainly into two nucleons then  $X_1$  is a neutron and the mass  $M_{X_1}$  is equal to the neutron mass  $m_n$ . If the value of  $M_{X_1}$ , obtained from the experiment, differs essentially from  $m_n$  then  $X_1 = \gamma + n$  and we have the additional indication that the observed dibaryon is the SND.

The simulation of the missing mass  $M_{X_1}$  spectra of the reaction  $pd \rightarrow ppX_1$  has been performed [16–18] assuming that the SND decays as  $D \rightarrow \gamma + {}^{31}S_0 \rightarrow \gamma pn$  through two nucleon singlet state  ${}^{31}S_0$  [6, 15, 18]. As a result, three narrow peaks at  $M_{X_1} = 965, 987, \text{ and } 1003$  MeV have been predicted. These peaks correspond to the decay of the isovector SNDs with masses 1904, 1926, and 1942 MeV, respectively.

In the experimental missing mass  $M_{X_1}$  spectrum besides the peak at the neutron mass caused by the process  $pd \rightarrow p + pn$ , three peaks have been observed at  $966 \pm 2, 986 \pm 2, \text{ and } 1003 \pm 2$  MeV [16–18]. These values of  $M_{X_1}$  coincide with the ones obtained by the simulation and essentially differ from the value of the neutron mass (939.6 MeV). Hence, for all states under study, we have  $X_1 = \gamma + n$  in support of the statement that the dibaryons found are SNDs.

On the other hand, the peak at  $M_{X_1} = 1003 \pm 2$  MeV corresponds to the peak found in ref. [19] and was attributed to an exotic baryon state  $N^*$  below the  $\pi N$  threshold. In that work the authors investigated the reaction  $pp \rightarrow \pi^+ X$  and have found altogether three such states with masses 1004, 1044, and 1094 MeV. Therefore, if the exotic baryons with anomalously small masses really exist, the observed peaks at 966, 986, and 1003 MeV might be a manifestation of such states. The existence of such exotic states, if proved to be true,

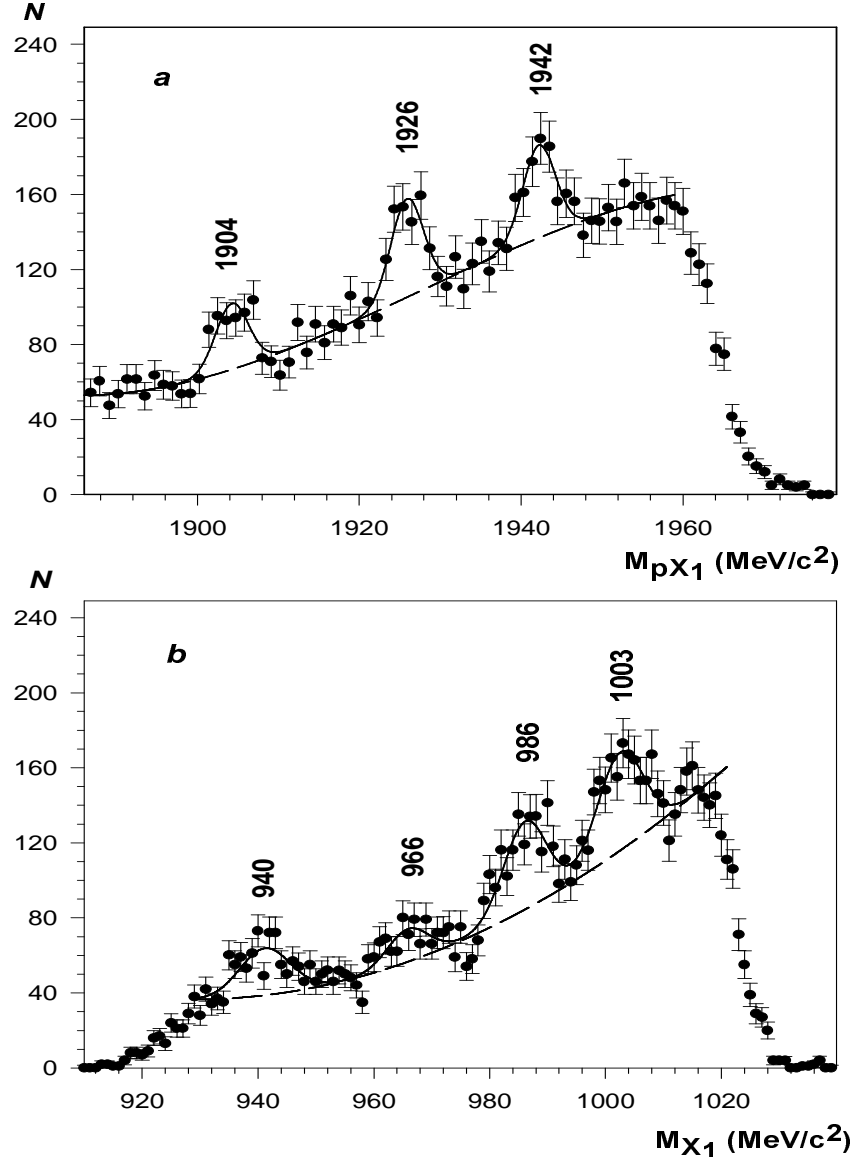


Figure 1: The missing mass  $M_{pX_1}$  (a) and  $M_{X_1}$  (b) spectra of the reaction  $pd \rightarrow p + pX_1$  for the sum of angles of  $\theta_R = 34^\circ$  and  $\theta_R = 36^\circ$ . The dashed and solid curves are results of interpolation by polynomials (for the background) and Gaussian (for the peaks), respectively.

will fundamentally change our understanding of the quark structure of hadrons [20, 21]. In ref. [22] these states were considered as possible candidates for pentaquark baryons consisted of  $u$  and  $d$  quarks.

However, the experiments on single nucleon have not observed any significant structure [23–25]. Therefore, the question about a nature of peaks observed in [18, 19] is open at present.

In ref. [26] dibaryons with exotic quantum numbers were searched for in the process  $pp \rightarrow pp\gamma\gamma$ . The experiment was performed with a proton beam from the JINR Phasotron at an energy of about 216 MeV. The energy spectrum of the photons emitted at  $90^\circ$  was measured. As a result, two peaks have been observed in this spectrum. This behavior of the photon energy spectrum was interpreted as a signature of the exotic dibaryon resonance  $d_1$  with a mass of about 1956 MeV and possible isospin  $T = 2$ . However, the result obtained in ref. [27] makes the possibility of production of dibaryons with  $T = 2$  in this reaction questionable. So, additional careful studies of the reaction  $pp \rightarrow pp\gamma\gamma$  are needed to understand more correctly the nature of the observed state.

On the other hand, an analysis [28] of the Uppsala proton-proton bremsstrahlung data looking for the presence of a dibaryon in the mass range from 1900 to 1960 MeV only gave the upper limits of 10 and 3 nb for the dibaryon production cross section at proton beam energies of 200 and 310 MeV, respectively. This result agrees with the estimates of the cross section obtained at the conditions of this experiment in the framework of the dibaryon production model suggested in ref. [15] and does not contradict the data of ref. [26].

Gerasimov [29, 30] suggested that a double radiative capture on the pionic deuterium ( $(\pi^-d)_{atom} \rightarrow nn\gamma\gamma$ ) is a candidate for the further investigation of the narrow dibaryons existence. The dibaryon in this reaction can be produced via the radiative capture  $\pi^-d \rightarrow \gamma d_1$  and then it decays to  $\gamma nn$ . Such an experiment has been carried out at the TRIUMF cyclotron using the beam of negative pions with a central momentum of 81.5 MeV/c [31]. No evidence for narrow dibaryons has been found in this work and a branching ratio upper limit,  $BR < 6.7 \times 10^{-6}$  (90% *C.L.*), for narrow  $d_1$  production in the mass region from 1920 to 1980 MeV was obtained. This upper limit is several order of magnitude below the yield estimate of Gerasimov ( $\sim 0.5\%$ ) obtained in a simple model [29]. However, if  $d_1$  is SND, this model does not really take into account a very strong overlap of the baryons which is a necessary condition of the SND production [6, 15, 18].

Let us make a crude estimation of the branching ratio of SND  $D(1, 1^\pm)$  production by a radiative capture on the pionic deuterium,  $BR((\pi^-d)_{atom} \rightarrow \gamma D(1, 1^\pm))$ , assuming that two neutrons in the reaction  $(\pi^-d)_{atom} \rightarrow nn$  mainly are in  ${}^{31}S_0$  state and using the model suggested in [6, 15, 18]. Then for the reaction  $(\pi^-d)_{atom} \rightarrow nn \rightarrow \gamma D(1, 1^\pm)$  we have

$$BR((\pi^-d)_{atom} \rightarrow \gamma D(1, 1^\pm)) \sim BR((\pi d)_{atom} \rightarrow nn)\alpha\eta_S$$

where  $BR((\pi^-d)_{atom} \rightarrow nn) \approx 0.74$  [32],  $\alpha$  is the fine-structure constant,  $\eta_S$  is the probability of the full overlap of two neutrons in  ${}^{31}S_0$  state. Using the experimental value of the SND production cross section in the process  $pd \rightarrow p + pX_1$  [18, 34], one has shown [33] that the probability of such an overlap of two nucleons in the deuteron ( $\eta$ ) is equal to  $\sim 10^{-4}$ . Supposing that also  $\eta_S \approx 10^{-4}$  we obtain

$$BR((\pi^-d)_{atom} \rightarrow \gamma D(1, 1^\pm)) \sim 0.74/137 \times 10^{-4} = 5.4 \times 10^{-7}.$$

This value is one order of magnitude below the upper limit obtained in [31].

The reactions  $pd \rightarrow pdX$  and  $pd \rightarrow ppX$  have been investigated also by Tamii *et al.* [34] at the Research Center for Nuclear Physics at the proton energy 295 MeV in the mass region of 1896–1914 MeV. They did not observe any narrow structure in this mass region and obtained the upper limit of the production cross section of a NN-decoupled dibaryon is equal to  $\sim 2 \mu\text{b}/\text{sr}$  if the dibaryon decay width  $\Gamma_D \ll 1$  MeV. And if  $\Gamma_D = 3$  MeV, the upper limit will be about  $3.5\mu\text{b}/\text{sr}$ . These limits are smaller than the value of the cross section of  $8 \pm 4\mu\text{b}/\text{sr}$  declared in ref. [15].

However, the latter value was overestimated that was caused by not taking into account angle fluctuations related to a beam position displacement on the  $\text{CD}_2$  target during the run. The beam displacement during a run decreased the efficiency for the elastic scattering and practically did not do that for the dibaryon formation reaction because of a wider cone of outgoing particles for the latter. As was shown in the next experimental runs, the real value of the cross sections of the production of the SND with the mass 1904 MeV must be smaller by 2–3 times than that was estimated in ref. [15].

On the other hand, simulation shows that the energy distribution of the protons from the decay of the SND with the mass of 1904 MeV is rather narrow with the maximum at  $\sim 74$  MeV. This distribution occupies the energy region of 60–90 MeV. The experiments [15, 18] confirmed the result of this simulation. However, in ref. [34] the authors considered the region 74–130 MeV. Therefore, they could detect only a small part of the SND contribution. Moreover, they used a very large angular acceptance of the spectrometer which detected these protons, while the protons under consideration have to fly in very narrow angle cone. As a result, the effect-to-background ratio in this experiment was more than 10 times less than in ref. [15, 18]. Very big errors and absence of proper proton energy and angular cuts in ref. [34] did not allow authors to observe any structure in the  $pX_1$  mass spectrum.

It is worth noting that the reaction  $pd \rightarrow NX$  was investigated in other works, too (see for example [35]). However, in contrast to the ref. [11–18], the authors of these works did not study either the correlation between the parameters of the scattered proton and the second detected particle or the emission of the photon from the dibaryon decay. Therefore, in these works the relative contribution of the dibaryons under consideration was small, which hampered their observation.

However, in order to argue more convincingly that the states found are really SNDs, an additional experimental investigation of the dibaryon production is needed.

On this point, the search for the SNDs in processes of the pion photoproduction from the deuteron is of great interest. Besides a decision of the question about an existence of the SNDs, an investigation of this process will allow the quantum numbers of the SNDs to be determined. And the experiment with the linear polarized photons will give possibility to determine other quantum numbers of the SNDs [8].

In ref. [36] narrow dibaryon resonances were searched for in the reaction  $\gamma d \rightarrow \pi^0 X$  in the photon energy region 140–300 MeV. No significant structure has been observed. Upper limits for the production of narrow dibaryons in the range 2–5  $\mu\text{b}$  averaged over the 0.8 MeV resolution has been observed. However, the expected values of the SND production cross section are essentially less. The estimation of the total cross section of the SND production in this process in the photon energy region 200–300 MeV (see sec. 3) gives 0.01–0.03  $\mu\text{b}$  for the dibaryon  $D(1, 1^+)$  with the mass 1904 MeV and it is less for the vector SND and the

higher masses.

Essentially bigger cross sections are expected for the SND production in the processes of the charged pion photoproduction.

We propose to search for the SNDs by studying the reactions  $\gamma d \rightarrow \pi^+ \gamma nn$ ,  $\gamma d \rightarrow \pi^- \gamma pp$ , and  $\gamma d \rightarrow \pi^0 \gamma pn$  in the photon energy region 300–800 MeV at MAMI. The mass of the SNDs will be reconstructed by the measurement of the photon and two nucleons. The detection of the pions will permit the background to be suppressed additionally. Using of a deuteron target allows avoiding uncertainties taken place in ref. [15–18,34] where CD<sub>2</sub> target was used. Furthermore, use of the photon beam with the energies of 300–800 MeV and the Crystal Ball spectrometer and TAPS will give a possibility to suppress essentially background and to investigate a wide mass spectrum and, particular, check the possibility of existence of the SNDs at  $M_{pX_1} = 1956$  [26] and 1982 MeV. The latter one was predicted in [18,33]. This experiment can also help to understand nature of the peaks in the  $M_{X_1}$  mass spectra and clarify a possibility of existence of exotic baryons with small masses.

## 2 The cross sections of the supernarrow dibaryon production in the reactions $\gamma d \rightarrow \pi D$

We will consider the following SNDs:  $D(T = 1, J^P = 1^+, S = 1)$  and  $D(1, 1^-, 0)$ .

It is worth noting that the state  $(T = 1, J^P = 1^-)$  corresponds to the states  ${}^{31}P_1$  and  ${}^{33}P_1$  in the NN channel. The former is forbidden and the latter is allowed for a two-nucleon state. In our work we will study the dibaryon  $D(1, 1^-, 0)$ , a decay of which into two nucleons is forbidden by the Pauli principle (i.e.  ${}^{31}P_1$  state).

In the process  $\gamma d \rightarrow pD$ , SNDs can be produced only if the nucleons in the deuteron overlap sufficiently, such that a 6-quark state with deuteron quantum numbers can be formed. In this case, an interaction of a photon or a meson with this state can change its quantum numbers so that a metastable state is formed. Therefore, the probability of the production of such dibaryons is proportional to the probability  $\eta$  of the 6-quark state existing in the deuteron.

The magnitude of  $\eta$  can be estimated from the deuteron form factor at large  $Q^2$  (see for example [37]). However, the values obtained depend strongly on the model of the form factor of the 6-quark state over a broad region of  $Q^2$ . Another way to estimate this parameter is to use the discrepancy between the theoretical and experimental values of the deuteron magnetic moment [38,39]. This method is free from the restrictions quoted above and gives  $\eta \leq 0.03$  [39]. In ref. [33] the magnitude of  $\eta$  was estimated by an analysis of the mass formula for SNDs using the experimental value of the cross section of the SND production in the process  $pd \rightarrow p + pX_1$  obtained in [18,34]. As a result,  $\eta \approx 10^{-4}$  has been obtained.

Since the energy of nucleons, produced in the decay of the SNDs under study with  $M < 2m_N + m_\pi$ , is small, it may be expected that the main contribution to a two nucleon system should come from the  ${}^{31}S_0$  (virtual singlet) state (Fig. 2). The results of calculations of the decay widths of the dibaryons into  $\gamma NN$  on the basis of such assumptions at  $\eta = 0.01$  are listed in Table 1. If  $\eta = 10^{-4}$ , the values of the decay widths would be smaller by  $\sim 10^2$

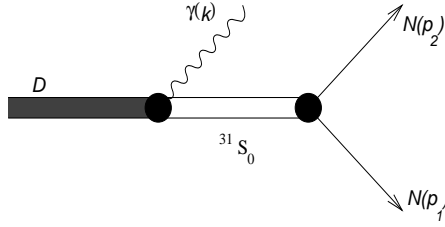


Figure 2: The diagram of the SND decay into  $\gamma NN$

Table 1: Decay widths of the dibaryons  $D(1, 1^+, 1)$  and  $D(1, 1^-, 0)$  at various dibaryon masses  $M$ .  $\Gamma_t \approx \Gamma_{\gamma NN}$

$M(\text{GeV})$	1.90	1.91	1.93	1.96	1.98	2.00	2.013
$\Gamma_t(1, 1^+)$ (eV)	0.51	1.57	6.7	25.6	48	81	109
$\Gamma_t(1, 1^-)$ (eV)	0.13	0.39	1.67	6.4	12	20	27

times. As a result of the SND decay through  ${}^3_1S_0$  in the intermediate state, the probability distribution of such a decay over the emitted photon energy  $\omega$  should be characterized by a narrow peak at the photon energy close to the maximum value  $\omega_m = (M^2 - 4m_N^2)/2M$  (Fig. 3). Note that the interval of the photon energy from  $\omega_m$  to  $\omega_m - 1$  MeV contains about 75% of the contribution to the width of the decay  $D(1, 1^\pm) \rightarrow \gamma NN$ . This leads to a very small relative energy of the nucleons from the SND decay ( $\lesssim 1$  MeV) and these nucleons will be emitted into a narrow angle cone with respect to the direction of the SND motion.

Let us calculate the cross section of the SND photoproduction. The gauge invariant amplitude of photoproduction of the SND dibaryon may be obtained with help of diagrams in Fig. 4.

Such a dibaryon could be produced only if a pion is emitted from the 6-quark state of the deuteron. Therefore the vertexes of  $d \rightarrow \pi D$  are written as

$$\Gamma_{d \rightarrow \pi D(1, 1^-, 0)} = \frac{g_1}{M} \sqrt{\eta} \Phi_{\mu\nu} G^{\mu\nu}, \quad (2)$$

$$\Gamma_{d \rightarrow \pi D(1, 1^+, 1)} = \frac{g_2}{M} \sqrt{\eta} \varepsilon_{\mu\nu\lambda\sigma} \Phi^{\mu\nu} G^{\lambda\sigma}, \quad (3)$$

where  $\Phi_{\mu\nu} = r_\mu w_\nu - w_\mu r_\nu$ ,  $G_{\mu\nu} = p_{1\mu} v_\nu - v_\mu p_{1\nu}$ ,  $w$  and  $v$  are 4-vectors of the dibaryon and deuteron polarization,  $r$  and  $p_1$  are the dibaryon and deuteron 4-momenta.

The following matrix elements correspond to the diagrams in Fig. 4a,b,c,d for the SND  $D(1, 1^-, 0)$

$$\begin{aligned} T_a &= -e\sqrt{\eta} \frac{g_1}{M} \frac{(\epsilon(2p_1 + k_1))}{(k_1 p_1)} \{(vw)(rP) - (vr)(wP)\} \\ T_b &= e\sqrt{\eta} \frac{g_1}{M} \frac{(\epsilon(2r - k_1))}{(k_1 r)} \{(vw)(p_1 Q) - (vQ)(p_1 w)\} \\ T_c(1^-) &= e\sqrt{\eta} \frac{g_1}{M} \frac{(\epsilon(2q - k_1))}{(k_1 q)} \{(vw)(p_1 r) - (vr)(p_1 w)\} \end{aligned} \quad (4)$$

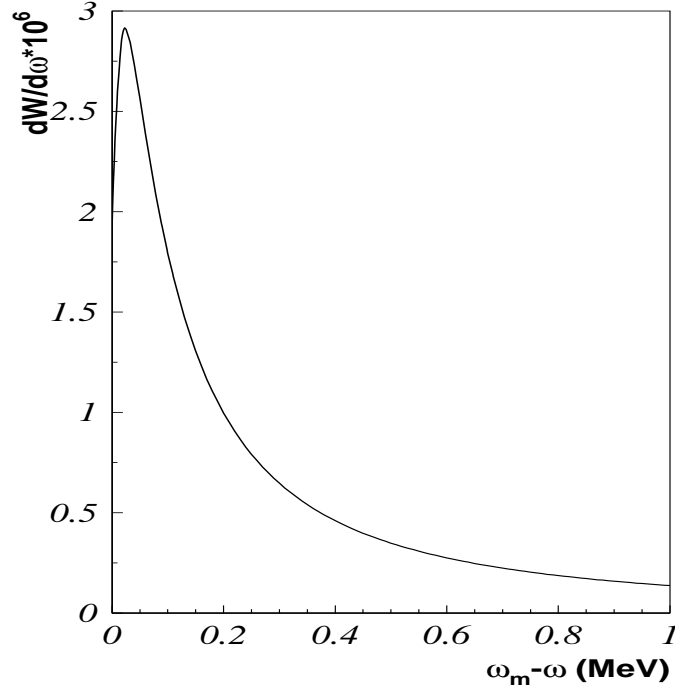


Figure 3: The distribution of the decay probability of the isovector SND over  $\omega_m - \omega$  at  $M = 1904$  MeV.

$$\begin{aligned}
T_d(1^-) &= T_{d1}(1^-) + \alpha T_{d2}(1^-) \\
T_{d1}(1^-) &= 2e\sqrt{\eta}\frac{g_1}{M} \{(vw)(\epsilon r) - (vr)(\epsilon w)\} \\
T_{d2}(1^-) &= 2e\sqrt{\eta}\frac{g_1}{M} \{(vw)(\epsilon p_1) - (\epsilon v)(p_1 w)\}
\end{aligned}$$

where  $P = (p_1 + k_1)$ ,  $Q = (r - k_1)$ ;  $k_1$  and  $q$  are the 4- momenta of the photon and the pion, respectively;  $\epsilon$  is the 4-vector of the photon polarization. The expression for the matrix element  $T_d$  is written in the form which ensures the gauge invariance of the amplitude of the dibaryon photoproduction. The coefficient  $\alpha$  is equal to 0, 1, 2 for the production of the  $\pi^+$ ,  $\pi^0$ ,  $\pi^-$  mesons, respectively.

For the SND  $D(1, 1^+, 1)$  we have

$$\begin{aligned}
T_a(1^+) &= 2e\sqrt{\eta}\frac{g_2}{M} \frac{(\epsilon(2p_1 + k_1))}{(k_1 p_1)} \epsilon_{\mu\nu\lambda\sigma} v^\mu w^\nu P^\lambda r^\sigma \\
T_b(1^+) &= -2e\sqrt{\eta}\frac{g_2}{M} \frac{(\epsilon(2r - k_1))}{(k_1 r)} \epsilon_{\mu\nu\lambda\sigma} v^\mu w^\nu p_1^\lambda Q^\sigma \\
T_c(1^+) &= -2e\sqrt{\eta}\frac{g_2}{M} \frac{(\epsilon(2q - k_1))}{(k_1 q)} \epsilon_{\mu\nu\lambda\sigma} v^\mu w^\nu p_1^\lambda r^\sigma \\
T_d(1^+) &= T_{d1}(1^+) + \alpha T_{d2}(1^+) \\
T_{d1}(1^+) &= -4e\sqrt{\eta}\frac{g_2}{M} \epsilon_{\mu\nu\lambda\sigma} v^\mu w^\nu \epsilon^\lambda r^\sigma
\end{aligned} \tag{5}$$

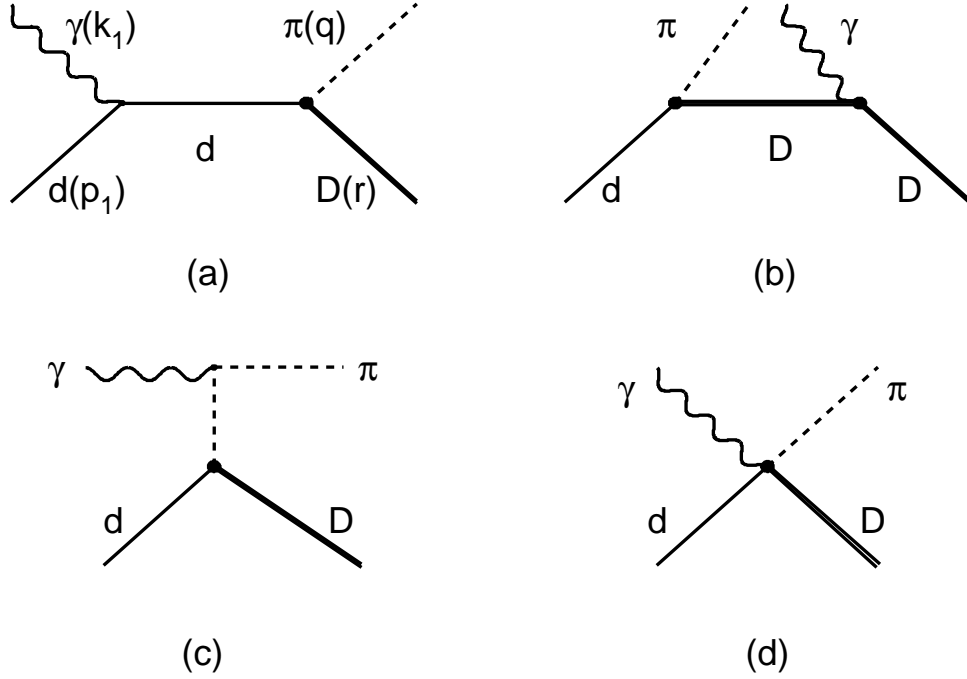


Figure 4: The diagrams of the SND production in the process  $\gamma d \rightarrow \pi D$

$$T_{d2}(1^+) = -4e\sqrt{\eta}\frac{g_2}{M}\varepsilon_{\mu\nu\lambda\sigma}v^\mu w^\nu p_1^\lambda \epsilon^\sigma$$

The matrix elements (4) and(5) are connected with the amplitudes of the SND photo-production in different channels as:

$$\begin{aligned} T(\gamma d \rightarrow \pi^0 D) &= T_a + T_b + T_{d1} + T_{d2} \\ T(\gamma d \rightarrow \pi^+ D) &= \sqrt{2}(T_a + T_c + T_{d1}) \\ T(\gamma d \rightarrow \pi^- D) &= -\sqrt{2}(T_a + 2T_b - T_c + T_{d1} + 2T_{d2}) \end{aligned} \quad (6)$$

Let us calculate the cross section of the dibaryon  $D(1, 1^-, 0)$  photoproduction in the reactions with formation of  $\pi^+$  meson. We will use the calibration  $\epsilon_0 = 0$ . Then the amplitude  $T_a$  is equal to zero in lab. system. As result of the calculation we have (in lab. system):

$$\begin{aligned} \frac{d\sigma_{\gamma d \rightarrow \pi^+ D(1^-)}}{d\Omega} &= \frac{1}{3} \left( \frac{e^2}{4\pi} \right) \left( \frac{g_1^2}{4\pi} \right) \eta \frac{q_1^2}{m_d M^2 \nu J} \left\{ \frac{1}{2m_d^2} [(M^2 + m_d^2 - t)^2 - 4m_d^2 M^2] + \right. \\ &\left. q_1^2 (1 - \cos^2 \theta) \left[ 1 + 2 \frac{(M^2 + m_d^2 - t)^2 + 2m_d^2 M^2}{(\mu^2 - t)^2} - 4 \frac{M^2 + m_d^2 - t}{\mu^2 - t} \right] \right\} \end{aligned} \quad (7)$$

where

$$s = 2m_d \nu + m_d^2, \quad t = \mu^2 - 2\nu(q_0 - q_1 \cos \theta_\pi), \quad J = q_1(m_d + \nu) - q_0 \nu \cos \theta_\pi,$$

$m_d$  is the deuteron mass,  $\nu$  is the incident photon energy,  $q_0(q_1)$  is the  $\pi$  meson energy (momentum). The pion energy  $q_0$  is connected with the pion emission angle  $\theta_\pi$  in the following way:

$$q_0 = \frac{1}{c_1} \left[ (m_d + \nu)c_2 + \nu \cos \theta_\pi \sqrt{c_2^2 - 2\mu^2 c_1} \right] \quad (8)$$

where

$$c_1 = 2[(m_d + \nu)^2 - \nu^2 \cos^2 \theta_\pi], \quad c_2 = s + \mu^2 - M^2.$$

The calculation of the cross section of the  $D(1, 1^+, 1)$  SND photoproduction has resulted in

$$\begin{aligned} \frac{d\sigma_{\gamma d \rightarrow \pi^+ D(1^+)}}{d\Omega} &= \frac{8}{3} \left( \frac{e^2}{4\pi} \right) \left( \frac{g_2^2}{4\pi} \right) \eta \frac{q_1^2}{m_d M^2 \nu J} \left\{ 2M^2 + \right. \\ &\left. q_1^2 (1 - \cos^2 \theta) \left[ 1 - 2 \frac{m_d^2 + M^2 - t}{\mu^2 - t} + \frac{(m_d^2 + M^2 - t)^2 - 4m_d^2 M^2}{(\mu^2 - t)^2} \right] \right\} \quad (9) \end{aligned}$$

For the  $D(1, 1^-, 0)$  and  $D(1, 1^+, 1)$  photoproduction in the process  $\gamma d \rightarrow \pi^- + D$  we have obtained:

$$\begin{aligned} \frac{d\sigma_{\gamma d \rightarrow \pi^- D(1^-)}}{d\Omega} &= \frac{1}{3} \left( \frac{e^2}{4\pi} \right) \left( \frac{g_1^2}{4\pi} \right) \eta \frac{q_1^2}{m_d M^2 \nu J} \left\{ \frac{1}{2} (M^2 + m_d^2 - t) \left( \frac{1}{m_d^2} + \frac{4}{M^2} \right) - \right. \\ &(M^2 + 4m_d^2) + q_1^2 (1 - \cos^2 \theta) \left[ 1 + \frac{A_1}{(M^2 - u)^2} + \frac{A_2}{(M^2 - u)} + \right. \\ &\left. \left. \frac{A_3}{(M^2 - u)(\mu^2 - t)} + \frac{A_4}{(\mu^2 - t)} + \frac{A_5}{(\mu^2 - t)^2} \right] \right\}, \quad (10) \end{aligned}$$

$$\begin{aligned} \frac{d\sigma_{\gamma d \rightarrow \pi^- D(1^+)}}{d\Omega} &= \frac{8}{3} \left( \frac{e^2}{4\pi} \right) \left( \frac{g_2^2}{4\pi} \right) \eta \frac{q_1^2}{m_d M^2 \nu J} \left\{ 2 [M^2 + 4m_d^2 - 4m_d r_0] + \right. \\ &q_1^2 (1 - \cos^2 \theta) \left[ 1 + 16 \frac{q_1^2 m_d^2}{(M^2 - u)^2} + 4 \frac{r_1^2 m_d^2}{(\mu^2 - t)^2} - 16 \frac{m_d^2 (q_0 r_0 - s + M^2 + \mu^2)}{(M^2 - u)(\mu^2 - t)} - \right. \\ &\left. \left. 8m_d (r_0 - 2m_d) \left( \frac{2}{(M^2 - u)} + \frac{1}{(\mu^2 - t)} \right) \right] \right\}, \quad (11) \end{aligned}$$

where

$$u = M^2 + m_d^2 + \mu^2 - s - t, \quad r_0 = m_d + \nu - q_0, \quad r_1 = \sqrt{r_0^2 - M^2},$$

$$\begin{aligned} A_1 &= 4 \left[ (m_d^2 - \mu^2 + u)^2 + 4m_d^2 u + \frac{(M^2 + m_d^2 - t)}{M^2} ((M^2 + u)(m_d^2 - \mu^2 + u) - \right. \\ &\left. u(M^2 + m_d^2 - t)) \right] \\ A_2 &= 4 \left[ 2(3m_d^2 - \mu^2 + u) - \frac{1}{M^2} (s - m_d^2)(M^2 + m_d^2 - t) \right] \\ A_3 &= 8 [(m_d^2 - \mu^2 + u)(M^2 + m_d^2 - t) + m_d^2 (M^2 + u)] \\ A_4 &= 4(M^2 + 3m_d^2 - t) \\ A_5 &= 2 [(m_d^2 + \mu^2 - t)^2 + 2m_d^2 M^2]. \quad (12) \end{aligned}$$

The calculation of the  $D(1, 1^-, 0)$  and  $D(1, 1^+, 1)$  production in the process  $\gamma d \rightarrow \pi^0 + D$  has given:

$$\frac{d\sigma_{\gamma d \rightarrow \pi^0 D(1^-)}}{d\Omega} = \frac{1}{6} \left( \frac{e^2}{4\pi} \right) \left( \frac{g_1^2}{4\pi} \right) \eta \frac{q_1^2}{m_d M^2 \nu J} \left\{ \frac{1}{2} (M^2 + m_d^2 - t) \left( \frac{1}{m_d^2} + \frac{1}{M^2} \right) - 2 (M^2 + m_d^2) + q_1^2 (1 - \cos^2 \theta) \left[ 1 + \frac{A_1}{4(M^2 - u)^2} + \frac{A_6}{(M^2 - u)} \right] \right\} \quad (13)$$

$$\frac{d\sigma_{\gamma d \rightarrow \pi^0 D(1^+)}}{d\Omega} = \frac{4}{3} \left( \frac{e^2}{4\pi} \right) \left( \frac{g_2^2}{4\pi} \right) \eta \frac{q_1^2}{m_d M^2 \nu J} \left\{ (M^2 + m_d^2 + t) + q_1^2 (1 - \cos^2 \theta) \left[ 1 + \frac{4q_1^2 m_d^2}{(M^2 - u)^2} + \frac{2(M^2 - m_d^2 - t)}{(M^2 - u)} \right] \right\}, \quad (14)$$

and

$$A_6 = 4(2m_d^2 - \mu^2 + u) - \frac{(M^2 + m_d^2 - t)}{M^2} (s - m_d^2).$$

The constants  $g_1^2/4\pi$ ,  $g_2^2/4\pi$ , and  $\eta$  are unknown. However, the product of these coupling constants and  $\eta$  can be estimated from the results of works [18, 34] where the SNDs were searched for in the process  $pd \rightarrow ppX_1$ . As a result we have

$$\eta \frac{g_1^2}{4\pi} = 0.7 \times 10^{-3}, \quad \eta \frac{g_2^2}{4\pi} = 1.5 \times 10^{-3}. \quad (15)$$

### 3 Kinematics of SND Photoproduction

We will consider SND with the masses  $M$  in the region 1900–2000 MeV.

Results of the calculations of the total and differential cross sections of the  $D(1, 1^-, 0)$  and  $D(1, 1^+, 1)$  production in the processes of the charged and neutral pion photoproduction from the deuteron are presented in Figs. 5 – 10.

The total cross sections of the  $D(1, 1^-, 0)$  production in the reaction with the  $\pi^+$  meson formation (Fig. 5) change from 50 nb up to 160 nb in the photon energy interval under consideration. The main contribution to the differential cross sections is given by the pions emitted to the angular region  $0^\circ \div 100^\circ$  with maximum at  $10^\circ - 30^\circ$ .

The total cross sections of the  $D(1, 1^+, 1)$  photoproduction in this reaction are equal to  $\sim 50$  nb (Fig. 6).

In the case of the  $\pi^-$  meson photoproduction, the total cross sections of the  $D(1, 1^-, 0)$  and  $D(1, 1^+, 1)$  production are bigger and reach for  $M = 1904$  MeV to 225 nb and 110 nb, respectively (Fig. 7, 8).

The values of the total cross sections of the  $D(1, 1^+, 1)$  production in the reaction  $\gamma d \rightarrow \pi^0 D$  are significantly less and are equal to 15 – 22 nb in the maximum (Fig. 9). However, the detection efficiency of the  $\pi^0$  meson photoproduction by the Crystal Ball Spectrometer and TAPS is higher than it for the charged pions and, therefore, the good yields are expected in this case. The angular distribution of the  $\pi^0$  mesons for this process is wider and occupies a region from  $0^\circ$  to  $180^\circ$ . The cross sections of  $D(1, 1^-, 0)$  production in the reaction under consideration are less by one order (Fig. 10).

So, the comparison of the SND photoproduction cross sections in the reactions with the formation of  $\pi^+$ ,  $\pi^-$ , and  $\pi^0$  mesons allows the quantum numbers of the SND to be determined.

Distributions of kinematical variables for the reaction under study are presented in Figs. 11, 12 for the SND masses 1900, 1950 and 2000 *MeV*.

Fig. 11 demonstrates the expected distributions of the nucleons over the energy and the emission angle. As seen from Fig. 11a,c,e, the nucleon energy is mainly smaller than 100 MeV. Therefore, we will limit ourselves by a consideration of the nucleon with such an energy. It will permit us to suppress the background essentially. The distribution over  $\cos\theta_n$  in Fig. 11b,d,f corresponds to an interval of the nucleon energy from 10 to 100 MeV and shows that nucleons will be emitted mainly to the angles  $0^\circ - 75^\circ$ .

Fig. 12 demonstrates distributions over the energy of the photon from the dibaryon decay and over  $\cos\theta_{\gamma n}$ , where  $\theta_{\gamma n}$  is an angle between the nucleon and the final photon. These distributions were obtained also for the nucleon energy in the interval 10 – 100 MeV.

## 4 Experimental setup

We propose to use the Crystal Ball (CB) spectrometer and TAPS detector system (CBTAPS) for the detection of all particles which are needed for the identification of the narrow six-quark states. The 5 cm long liquid hydrogen or deuterium target surrounded by inner detectors is located inside the CB. Experimental setup is shown schematically in Fig. 13. To show the inner detectors, the upper hemisphere of the CB is omitted.

The CB is constructed of 672 NaJ(Tl) crystals with 15.7 radiation length thick. The crystals are arranged in a spherical shell with an inner radius of 25.3 cm and an outer radius of 66.0 cm. The CB has an entrance and exit opening for the beam.

The inner detectors include two coaxial cylindrical multiwire proportional chambers (MWPC), developed early for the DAPHNE detector [40], and a cylindrically arranged plastic scintillator particle-identification detector (PID) [41] placed between the MWPC and the target. The MWPC will be used as a charge particle tracker. The PID will be used, from one side, as a  $\Delta E$ -detector to separate pions and protons and, from other side, as a "Veto" for charged particles when photons in the CB are detected.

The TAPS detector [42, 43] is implemented as a forward wall at 1.8 m from the target. It comprises 510 BaF<sub>2</sub> hexagonally shaped crystals with 12 radiation length thick. A hexagonal plastic scintillator detector (5 mm thick) with an individual photomultiplier readout is mounted in the front of each crystal. It acts as "Veto" for charged particles when photons or neutrons are detected in the TAPS. The 1.8 m distance between the TAPS and the target is quite enough to separate pions and protons using time of flight of the particle and its total energy absorption in the TAPS. Besides we will be able to identify neutrons and calculate theirs energy by the time of flight. High granularity of the TAPS provides a good tracking for both charge and neutral particles.

The described experimental setup is now available in the experimental hall of the A2 collaboration at the continuous-wave electron accelerator MAMI B [44, 45]. The Glasgow-Mainz photon tagging facility [46, 47], which provides photon beam for A2 collaboration experiments, can tag bremsstrahlung photons in the energy range 40-820 MeV with an

intensity  $\sim 0.6 \times 10^6 \gamma/s$  in the lowest photon energy tagger channel. The average energy resolution is 2 MeV.

## 5 Background

The charged and neutral particles CBTAPS detector combined with the Glasgow-Mainz tagging facility is a very advantageous instrument to search for and investigate the narrow six-quark states in the pion photoproduction reactions. For this experimental setup an optimal way to recognize the narrow six-quark states is a reconstruction of invariant mass for three particles detected: photon and two nucleons. To suppress the background contribution to this spectrum it is necessary to additionally detect the pion, neutral or charged, depending on the reaction channel.

The main anticipated background reactions are

$$\begin{aligned}\gamma + d &\rightarrow \pi^0 + \pi^+ + n + n, \\ \gamma + d &\rightarrow \pi^0 + \pi^- + p + p, \\ \gamma + d &\rightarrow \pi^0 + \pi^0 + p + n'\end{aligned}\tag{16}$$

and

$$\gamma + d \rightarrow \pi + \gamma + N + N.\tag{17}$$

The double pion production reactions are important for the photon energies more than 500 MeV and only in the case when one of the photons from the  $\pi^0$  decay is not detected. But the  $\pi^0$  detection efficiency for CBTAPS detector is over 85% and it will reject most of this background. Because we detect all secondary particles involved we can apply a lot of different kinematic cuts which will further suppress these processes. The process (17) has the value of the total cross section similar to the one under study. However, this background is distributed over full mass region, whereas the SND photoproduction gives contribution in a narrow region about the six-quark state mass.

## 6 GEANT simulation

To estimate expected yields for the SND formation we performed Monte-Carlo simulation based on GEANT3 code [48], in which all relevant properties of the setup are taken into account. Initial distributions for the event generator included differential cross sections of the SND production calculated according to sec. 2. The distribution of the SND decay probability (see Fig. 3) is also taken into account. Besides the following beam conditions were used

- Incoming electron beam energy: 880 MeV.
- Tagged photon energy range: 300 – 820 MeV.
- Maximal count rate in the tagger:  $6 \times 10^5$  1/s.
- Tagging efficiency: 50%.

$M$ (MeV)	$\gamma d \rightarrow \pi^+ D(1, 1^-)$		$\gamma d \rightarrow \pi^- D(1, 1^-)$		$\gamma d \rightarrow \pi^0 D(1, 1^+)$	
	yields	$\sigma_M$	yields	$\sigma_M$	yields	$\sigma_M$
1904	380	4.0	4720	4.0	1300	3.8
1926	460	4.6	5270	4.6	1350	4.4
1942	480	5.7	5120	5.5	1340	5.6
1980	560	6.9	4830	7.0	1180	6.9

Table 2: Expected yields of the SNDs and the mass resolutions ( $\sigma_M$  (MeV))

The results of the GEANT simulation of the invariant  $\gamma NN$  mass spectra for the production of the isovector SNDs with masses 1904, 1926, 1942, and 1980 MeV for the processes of the pion photoproduction from the deuteron are presented in Fig. 14 for 300 hours of the beam time. The productions of  $D(1, 1^-)$  in the reactions  $\gamma d \rightarrow \pi^+ \gamma nn$  and  $\gamma d \rightarrow \pi^- \gamma pp$  are shown in Fig. 14a and 14b, respectively. Fig. 14c shows the invariant  $\gamma pn$  mass spectrum for the  $D(1, 1^+)$  in the process of  $\pi^0$  meson photoproduction from the deuteron. As seen from Fig 14, it is expected that the SND can be easily extracted from the experimental data with the number of standard deviations more than 10.

If SNDs really exist then, besides the peaks in  $\gamma NN$  spectra, we must also observe the corresponding peaks in  $\gamma p$  and  $\gamma n$  mass spectra which are connected with the dynamic of the SNDs decay. Such spectra, obtained in the GEANT simulation, are represented in Fig. 15 for the process  $\gamma d \rightarrow \pi^0 D(1, 1^+)$ ,  $D(1, 1^+) \rightarrow \gamma pn$  and in Fig. 16 for  $\gamma d \rightarrow \pi^- D(1, 1^-)$ ,  $D(1, 1^-) \rightarrow \gamma pp$ . Figs. 15a and 16a demonstrate the spectra without an influence of the detectors and Figs. 15b and 16b with an influence of the detectors. The observation of the peaks in the  $\gamma N$  mass spectra is the necessary condition to prove the SND existence.

The spectra in Figs. 15a and 16a were obtained assuming that SNDs decay without of the  $N^*$  production. As a result, the widths of the peaks in these figures are about a few MeV. If the exotic baryons  $N^*$  exist, their decay widths have to be  $\ll 1$  MeV. Therefore, experiments with the mass resolution  $\lesssim 1$  MeV can give a conclusion about the existence of the exotic baryons  $N^*$  with the small masses.

The expected yields of the SNDs as a result of the simulation of the isovector SND production in the processes of the pion photoproduction from the deuteron at the Mainz microtron MAMI in the photon energy region 300–820 MeV for the beam time of 300 hours are listed in table 2 for the different masses of SNDs. The expected mass resolution  $\sigma_M$  are presented here too. As seen from this table the biggest yield of  $D(1, 1^-)$  is expected in the process of the  $\pi^-$  meson photoproduction. The photoproduction of  $\pi^0$  meson results mainly in the  $D(1, 1^+)$  formation. So investigation of the considered in this work processes give possibility both to observe the SNDs and determine their quantum numbers.

## 7 Summary

- A search for narrow six-quark states in the reactions  $\gamma d \rightarrow \pi^+ \gamma nn$ ,  $\gamma d \rightarrow \pi^- \gamma pp$ , and  $\gamma d \rightarrow \pi^0 \gamma pn$  at MAMI-B is proposed.
- The masses of the SNDs will be reconstructed by a measurement of the photon and two nucleon.
- Using of the deuteron target allows avoiding uncertainties taken place in the experiment at INR.
- Using of the Crystal Ball spectrometer and TAPS allows one to detect  $\gamma$ ,  $p$  and  $n$  with good accuracy and suppress essentially the background.
- This experiment will give possibility to observe the SNDs in the mass region from 1880 up to 2000 MeV with good enough precision.
- A comparison of the results obtained for the reactions under study will allow the quantum numbers of the SNDs ( $T$ ,  $J^P$ ) to be determined.
- Study of the  $\gamma p$  and  $\gamma n$  mass spectra will give an additional information about the nature of the observed dibaryon states and a possibility of existence of exotic baryons with small masses.

## References

- [1] R.L. Jaffe, Phys.Rev.Lett. **38**, 195 (1977); P.J.G. Mulders, A.T. Aerts, and J.J. de Swart, Phys.Rev.Lett. **40**, 1543 (1978); D.B. Lichtenberg, E. Predazzi, D.H. Weingarten, and J.G. Wills, Phys.Rev. **D18**, 2569 (1978); V. Matveev and P. Sorba, Lett.Nuovo Cim. **20**, 435 (1977).
- [2] P.J.G. Mulders, A.T.M. Aerts, and J.J. de Swart, Phys. Rev. D **21** 2653 (1980).
- [3] B. Tatischeff, J. Yonnet, M. Boivin, M.P. Comets, P. Courtat, R. Gacougnolle, Y. Le Bornec, E. Loireleux, F. Reide, and N. Willis, Phys. Rev. C **59**, 1878 (1999).
- [4] L.V. Fil'kov, Sov.Physics–Lebedev Inst. Reports No.11, 49 (1986); Sov.J.Nucl.Phys. **47**, 437 (1988).
- [5] D.M. Akhmedov *et al.*, Proceed. of the 8th Seminar "Electromagnetic interactions of nuclei at low and medium energies", Moscow, (1991), p.228; *ibid*, p.252.
- [6] D.M. Akhmedov and L.V. Fil'kov, Nucl.Phys. **A544**, 692 (1992).
- [7] V.M. Alekseyev, S.N. Cherepnya, L.V. Fil'kov, and V.L. Kashevarov, Preprint of Lebedev Phys.Inst., No 52 (1996).
- [8] V.M. Alekseyev, S.N. Cherepnya, L.V. Fil'kov, and V.L. Kashevarov, Kratkie Soobsheniya po fizike, FIAN, No.1, 28 (1998); nucl-th/9812041.
- [9] V.B. Kopeliovich, Phys.At.Nucl. **56**, 1084 (1993); **58**, 1237 (1995).
- [10] T. Krupnovnickas, E. Norvaišas, and D.O. Riska, Lithuanian J. Phys. **41**, 13 (2001); nucl-th/0011063.
- [11] L.V. Fil'kov, E.S. Konobeevski, M.V. Mordovskoy, S.I. Potashev, and V.M. Skorkin, Preprint of INR, No. 0923/96 (1996).
- [12] E.S. Konobeevski, M.V. Mordovskoy, S.I. Potashev, V.M. Skorkin, S.K. Zuev, V.A. Simonov, and L.V. Fil'kov, Izv. Ross. Akad. Nauk, Ser. Fiz. **62**, 2171 (1998).
- [13] L.V. Fil'kov, V.L. Kashevarov, E.S. Konobeevskiy, M.V. Mordovskoy, S.I. Potashev, and V.M. Skorkin, Bulletin of Lebedev Phys. Inst. No **11**, 36 (1998).
- [14] L.V. Fil'kov, V.L. Kashevarov, E.S. Konobeevskiy, M.V. Mordovskoy, S.I. Potashev, and V.M. Skorkin, Phys. Atom. Nucl. **62**, 2021 (1999).
- [15] L.V. Fil'kov, V.L. Kashevarov, E.S. Konobeevski, M.V. Mordovskoy, S.I. Potashev, and V.M. Skorkin, Phys. Rev. C **61**, 044004 (2000).
- [16] L.V. Fil'kov, V.L. Kashevarov, E.S. Konobeevskiy, M.V. Mordovskoy, S.I. Potashev, V.A. Simonov, V.M. Skorkin, and S.V. Zuev, VII Conf. CIPANP2000, Quebec City, Canada, 22-28 May 2000, AIP Conf. Proceed. v.**549**, p.267; nucl-th/0009044.

- [17] L.V. Fil'kov, V.L. Kashevarov, E.S. Konobeevskiy *et al.*, Proceed. XV Intern. Seminar on High Energy Physics "Nuclear Physics and Quantum Chromodynamics", Dubna, 25-29 September, 2000, v.**II**, p.153, nucl-th/0101021; Proceed. 9th Intern. Conf. on Hadron Spectroscopy, Protvino, Russia 25 August–1 September 2001, AIP Conference Proceedings, v.**619**, p.753.
- [18] L.V. Fil'kov, V.L. Kashevarov, E.S. Konobeevski, M.V. Mordovskoy, S.I. Potashev, V.A. Smirnov, V.M. Skorkin, and S.V. Zuev, Eur. Phys. J. A **12**, 369 (2001).
- [19] B. Tatischeff, J. Yonnet, N. Willis, M. Boivin, M.P. Comets, P. Courtat, R. Gacougnolle, Y.Le Bornec, E. Loireleux, and F. Reide, Phys. Rev. Lett. **79**, 601 (1997).
- [20] L.V. Fil'kov, Proceed. of XVI Intern. Baldin Seminar on High-Energy Physics, Dubna, Russia, 10-15 June 2002, nucl-th/0208028; nucl-th/0307088.
- [21] Th. Walcher, hep-ph/0111279.
- [22] Ya.I. Azimov, R.A. Arndt, I.I. Strakovsky, and R.L. Workman, nucl-th/0307088.
- [23] A.I. L'vov and R.L. Workman, Phys.Rev.Lett. **81**, 1346 (1998).
- [24] X. Jiang *et al.*, Phys.Rev. C **67**, 028201 (2003).
- [25] M. Kohl *et al.*, Phys.Rev. C **67**, 065204 (2003).
- [26] A.S. Khrykin, V.F. Boreiko, Yu.G. Budyashev, S.B. Gerasimov, N.V. Khomutov, Yu.G. Sobolev, and V.P. Zorin, Phys. Rev. C **64**, 034002 (2001).
- [27] Ya.I. Azimov and I.I. Strakovskiy, Sov.J.Nucl.Phys. **51**, 606 (1990).
- [28] H. Calén *et al.*, Phys.Lett. **B427**, 248 (1998).
- [29] S.B. Gerasimov, Proceed. of Intern. Workshop "Hadronic Atoms and Positronium in the Standart Model", Dubna, Russia, 26–31 May 1998, JINR-E2-98-254, Dubna 1998 p.91; nucl-th/9808070.
- [30] S.B. Gerasimov, Proceed. of XV Intern. Seminar on High Physics Problems, Dubna, Russia, 25–29 Sept. 2000, JINR-E1,2-2001-291, Dubna, 2001, Vol. II, p. 166.
- [31] P.A. Żolnierczuk *et al.*, Phys. Lett. B **549**, 301 (2000).
- [32] R. MacDonald *et al.*, Phys. Rev. Lett. **38**, 746 (1977); V.L. Highland *etal.*, Nucl. Phys. **B 365**, 333 (1981).
- [33] L.V. Fil'kov, nucl-th/0307076.
- [34] A. Tamii *et al.*, Phys. Rev. C **65**, 047001 (2002).
- [35] K.K. Set, Proc. XII Int. Conf. on Few Body Problems in Physics, Vancouver, Canada, TRIUMF, TR-89-2, C35; L.C. Bland, T.W. Bowyer, D.S. Carman, V. Derenchuk, D.L. Friesel, C.D. Goodman, A.H. Smith, J. Sowinski, S.E. Vigdor, and G. Xu, IUCF Scientific and Technical Report (1989-1990), p.14.

- [36] U. Siodlaczek, P. Achenbach, J. Ahrens *et al.*, Eur. Phys. J. A **9**, 309 (2000).
- [37] V.V. Burov, S.M. Dorkin, V.K. Lukyanov, and A.I. Titov, Z.Phys. **A306**, 149 (1982); I.L. Grash and L.A. Kondratyuk, Sov.J.Nucl.Phys. **39**, 198 (1984).
- [38] Y.E. Kim and M. Orłowski, Phys.Lett. **140B**, 275 (1984); R.K. Bhadury and Y. Nogami, Phys.Lett. **152B**, 35 (1985).
- [39] L.A. Kondratyuk, M.I. Krivoruchenko, and M.G. Shchepkin, Sov.J.Nucl.Phys. **43**, 899 (1986).
- [40] G.Audi *et al.*, Nucl. Inst. Meth. **A301**, 473 (1991).
- [41] D.P.Watts, Crystal Ball collaboration meeting, [www.physics.gla.ac.uk/~dwatts/pid.html](http://www.physics.gla.ac.uk/~dwatts/pid.html) (2003).
- [42] R. Novotny, IEEE Trans. Nucl. Scie. **38**, 379 (1991).
- [43] A.R. Gabler *et al.*, Nucl. Inst. Meth. **A346**, 168 (1994).
- [44] T. Walcher, Prog. Part. Nucl. Phys. **24**, 189 (1990).
- [45] J. Ahrens *et al.*, Nuclear Physics News **4**, 5 (1994).
- [46] I. Anthony *et al.*, Nucl. Inst. Meth. **A301**, 230 (1991).
- [47] S. Hall *et al.*, Nucl. Inst. Meth. **A368**, 698 (1996).
- [48] R. Brun, *et al.*, GEANT, Cern/DD/ee/84-1, 379 1986.

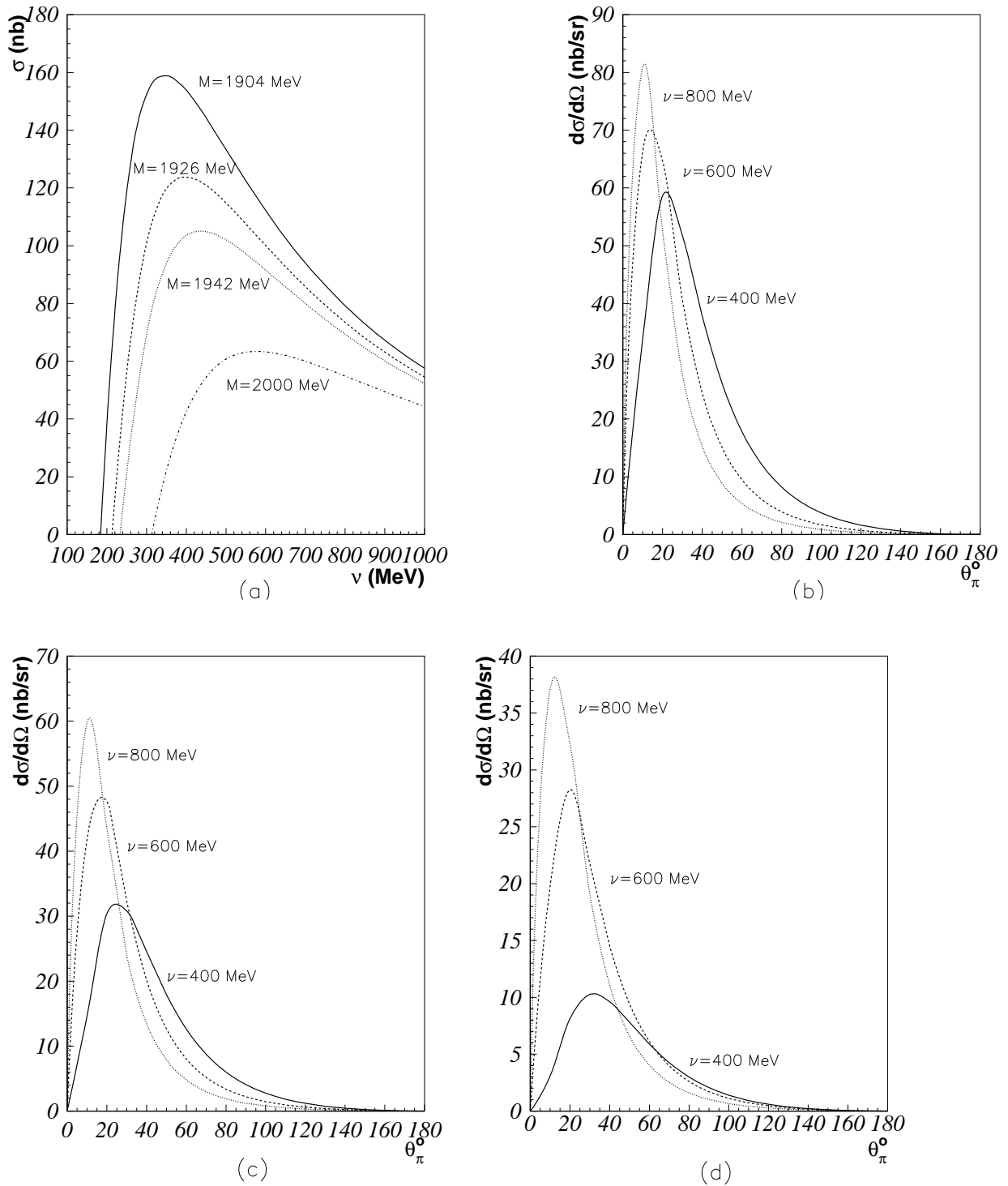


Figure 5: The cross sections of the SND  $D(1, 1^-, 0)$  production in the reaction  $\gamma d \rightarrow \pi^+ D$ ; (a) –the total cross sections; (b,c,d) – the differential cross sections for  $M = 1900, 1942,$  and  $2000$  MeV, respectively.

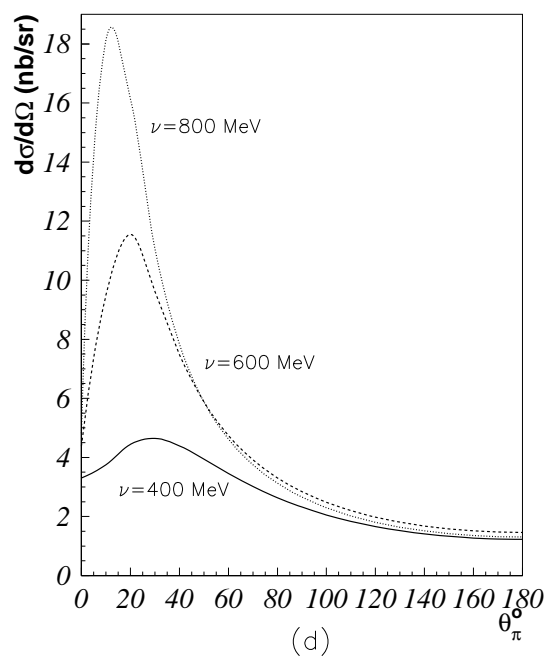
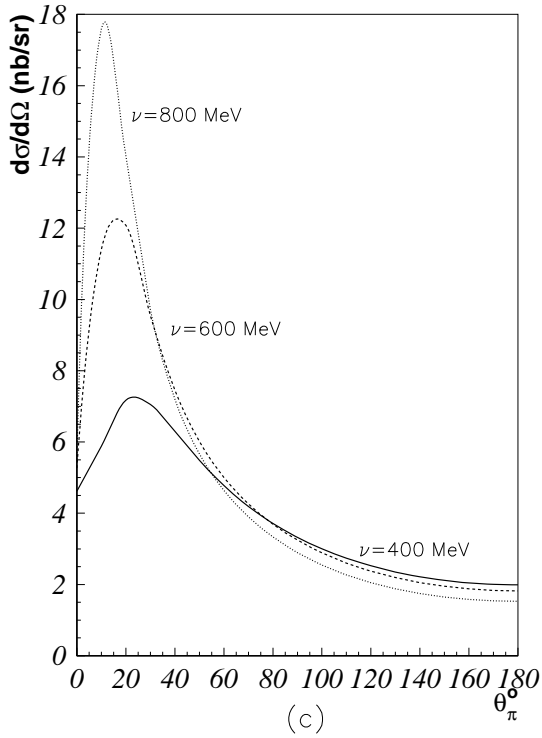
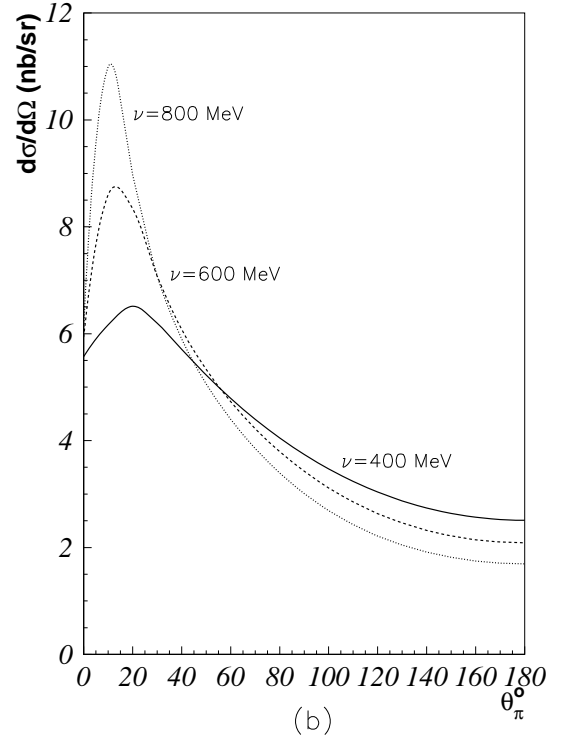
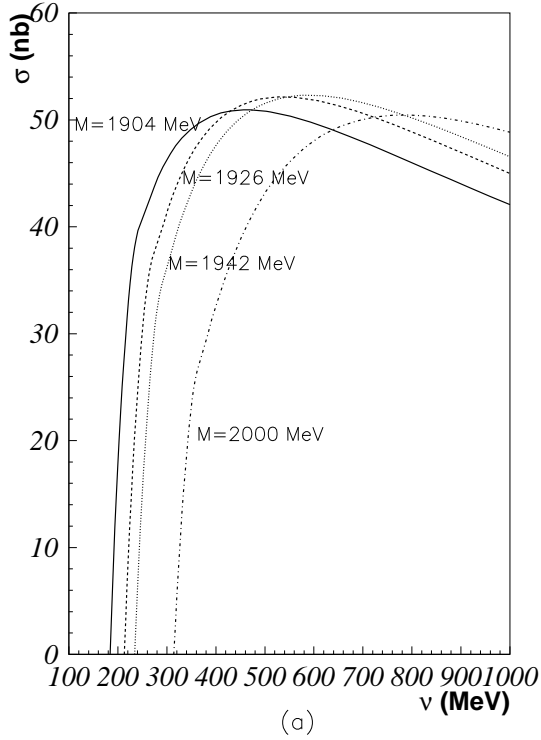


Figure 6: The cross sections of the SND  $D(1, 1^+, 1)$  production in the reaction  $\gamma d \rightarrow \pi^+ D$ ; (a) – the total cross sections; (b,c,d) – the differential cross sections for  $M = 1900, 1942,$  and  $2000$  MeV, respectively.

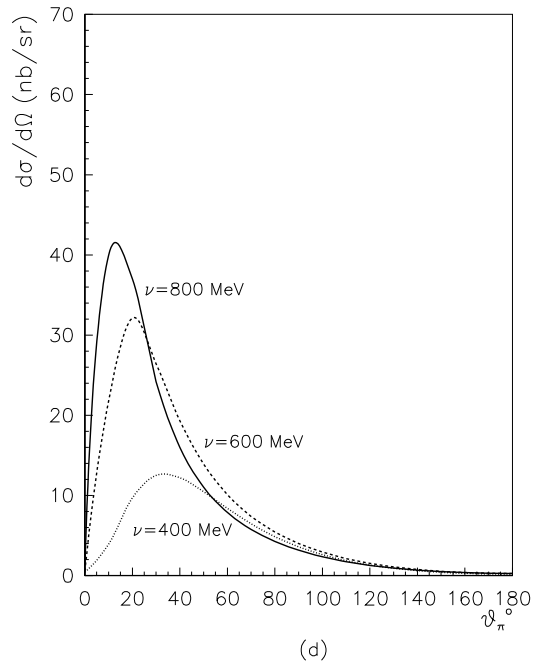
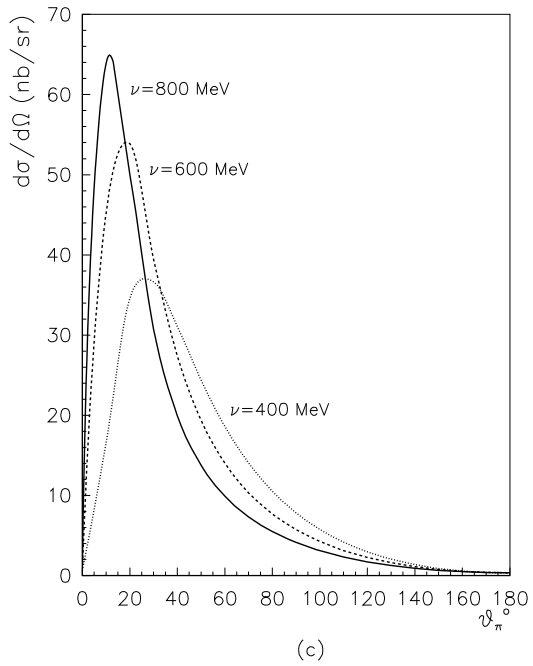
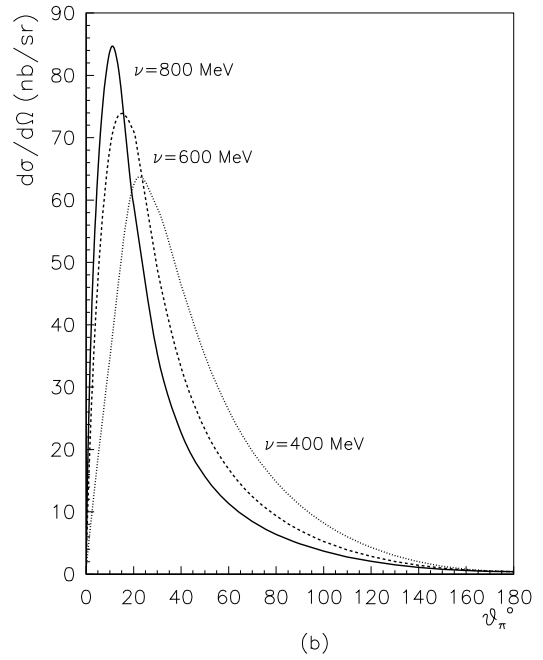
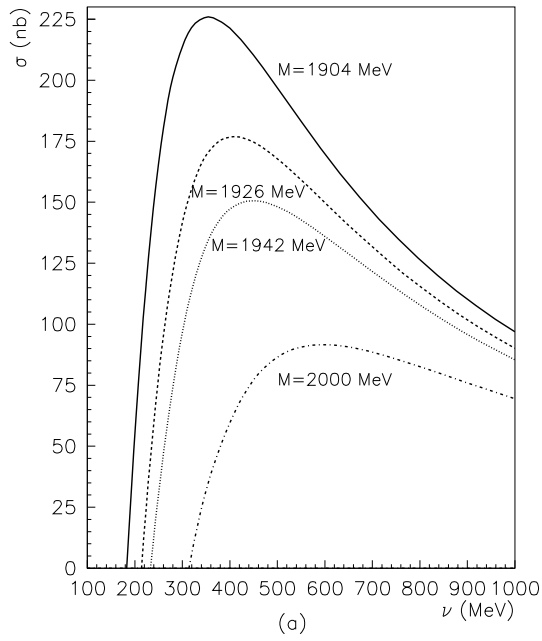


Figure 7: The cross sections of the SND  $D(1, 1^-, 0)$  production in the reaction  $\gamma d \rightarrow \pi^- D$ ; (a) –the total cross sections; (b,c,d) – the differential cross sections for  $M = 1904, 1942,$  and  $2000$  MeV, respectively.

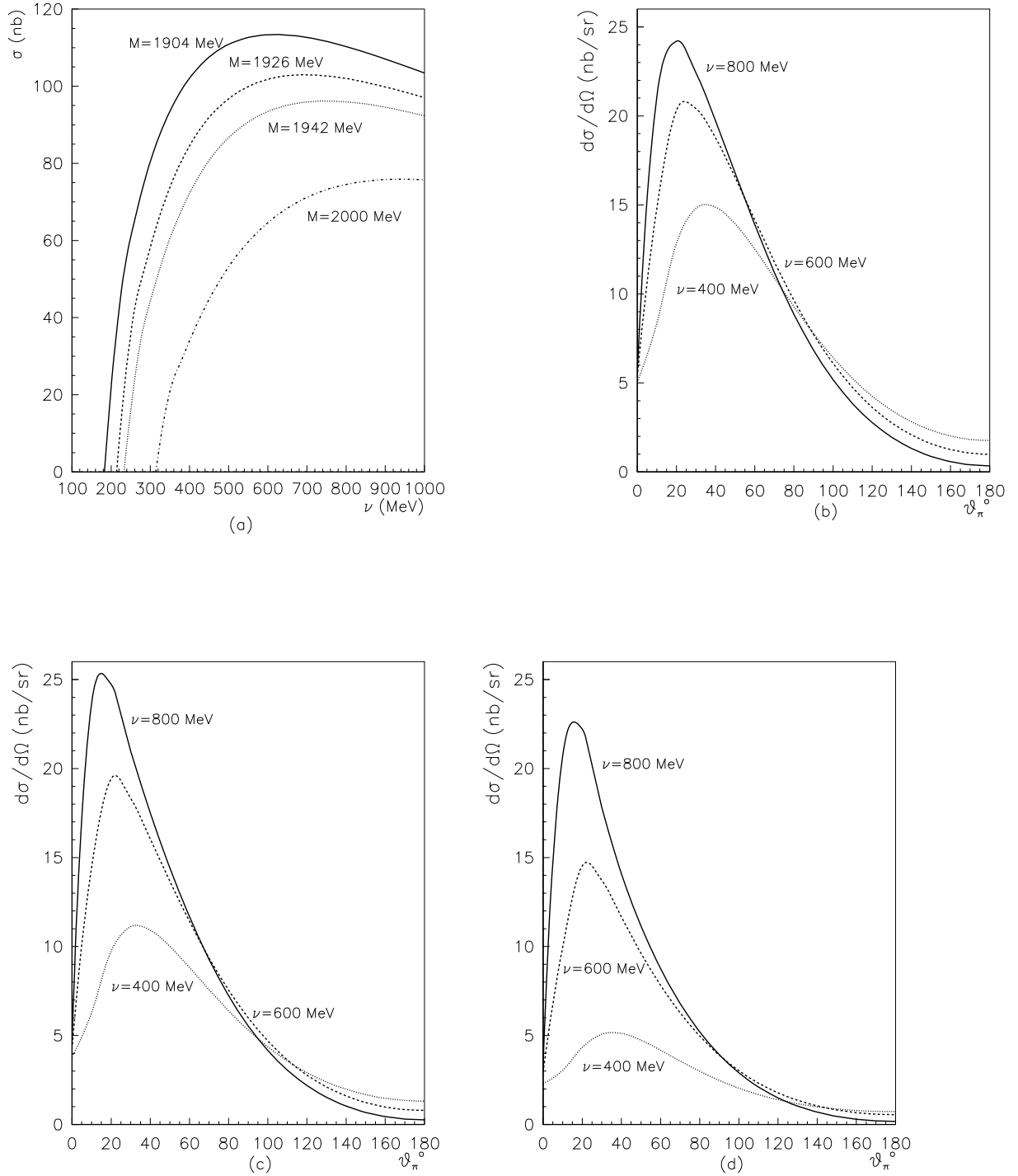


Figure 8: The cross sections of the SND  $D(1, 1^+, 1)$  production in the reaction  $\gamma d \rightarrow \pi^- D$ ; (a) –the total cross sections; (b,c,d) – the differential cross sections for  $M = 1904, 1942,$  and  $2000$  MeV, respectively.

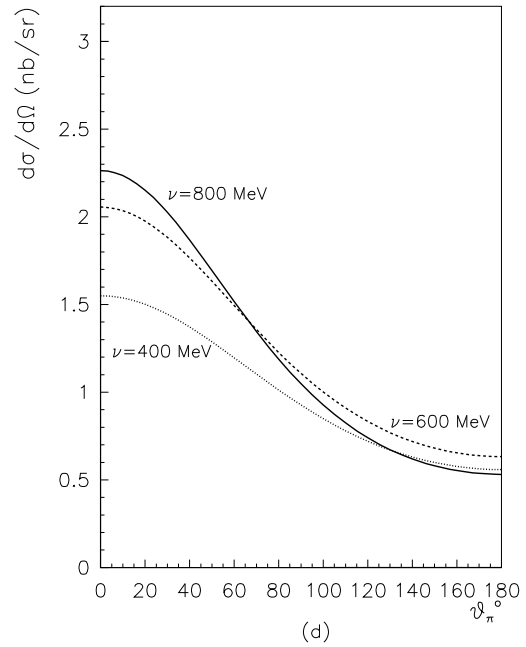
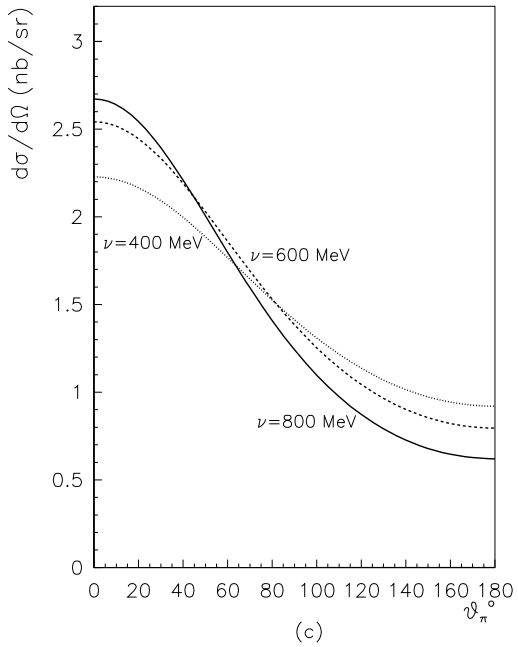
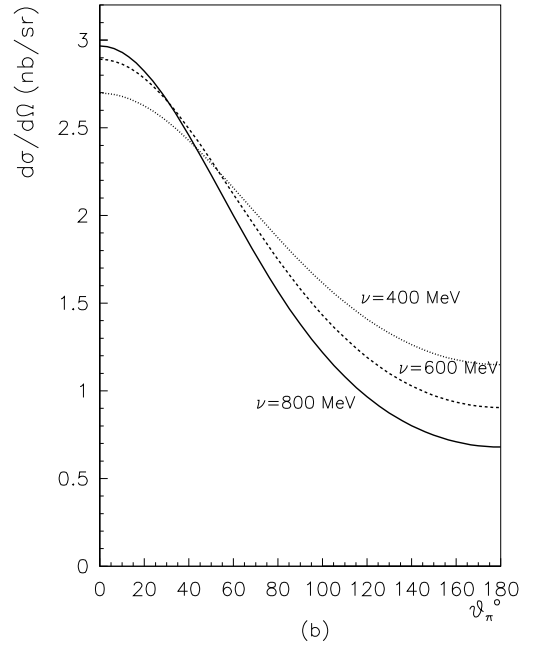
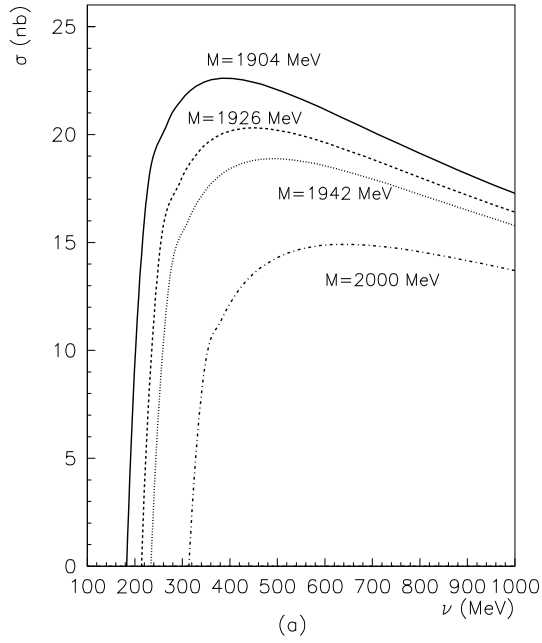


Figure 9: The cross sections of the SND  $D(1, 1^+, 1)$  production in the reaction  $\gamma d \rightarrow \pi^0 D$ ; (a) –the total cross sections; (b,c,d) – the differential cross sections for  $M = 1904, 1942,$  and  $2000$  MeV, respectively.

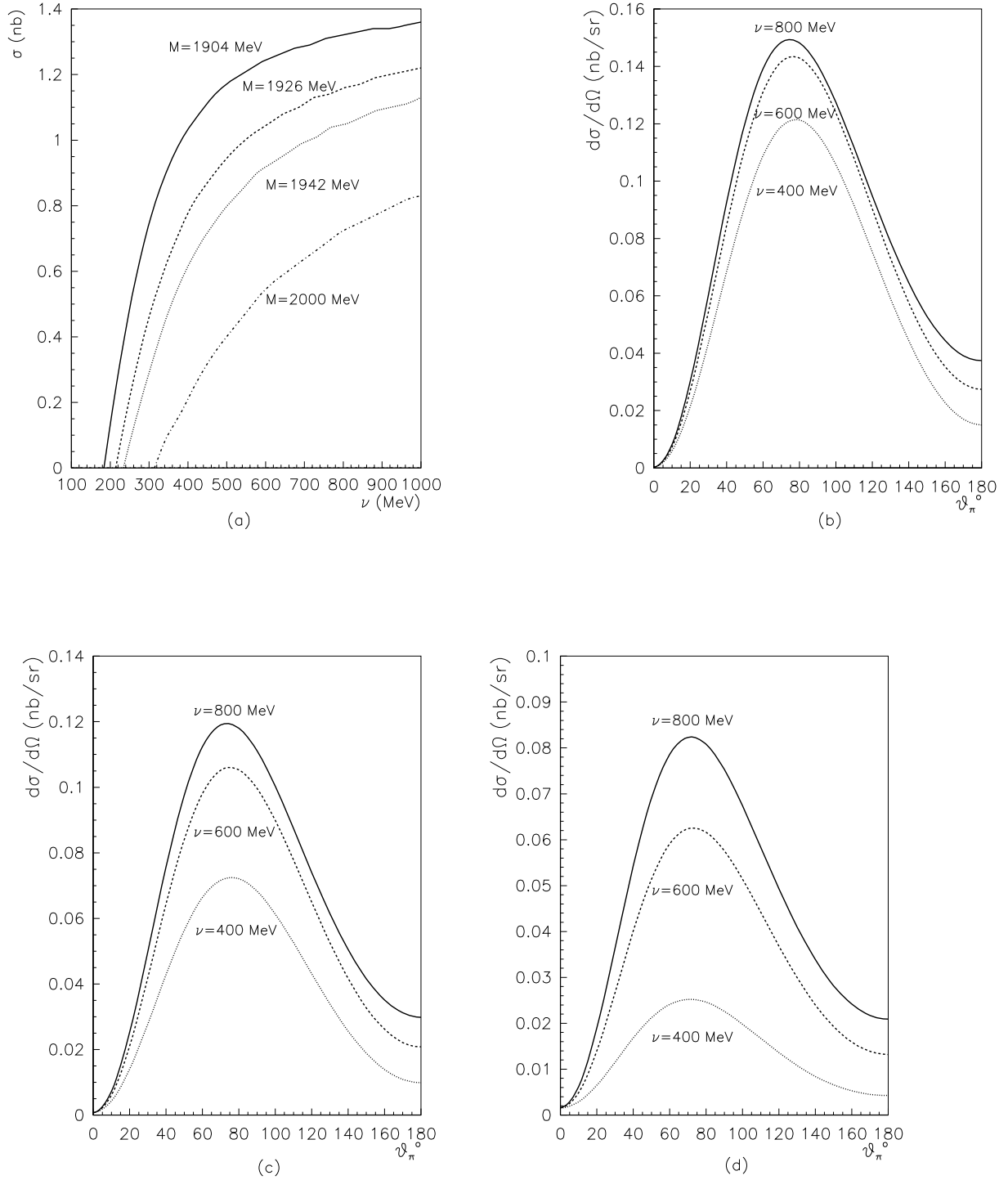


Figure 10: The cross sections of the SND  $D(1, 1^-, 0)$  production in the reaction  $\gamma d \rightarrow \pi^0 D$ ; (a) –the total cross sections; (b,c,d) – the differential cross sections for  $M = 1904, 1942,$  and  $2000$  MeV, respectively.

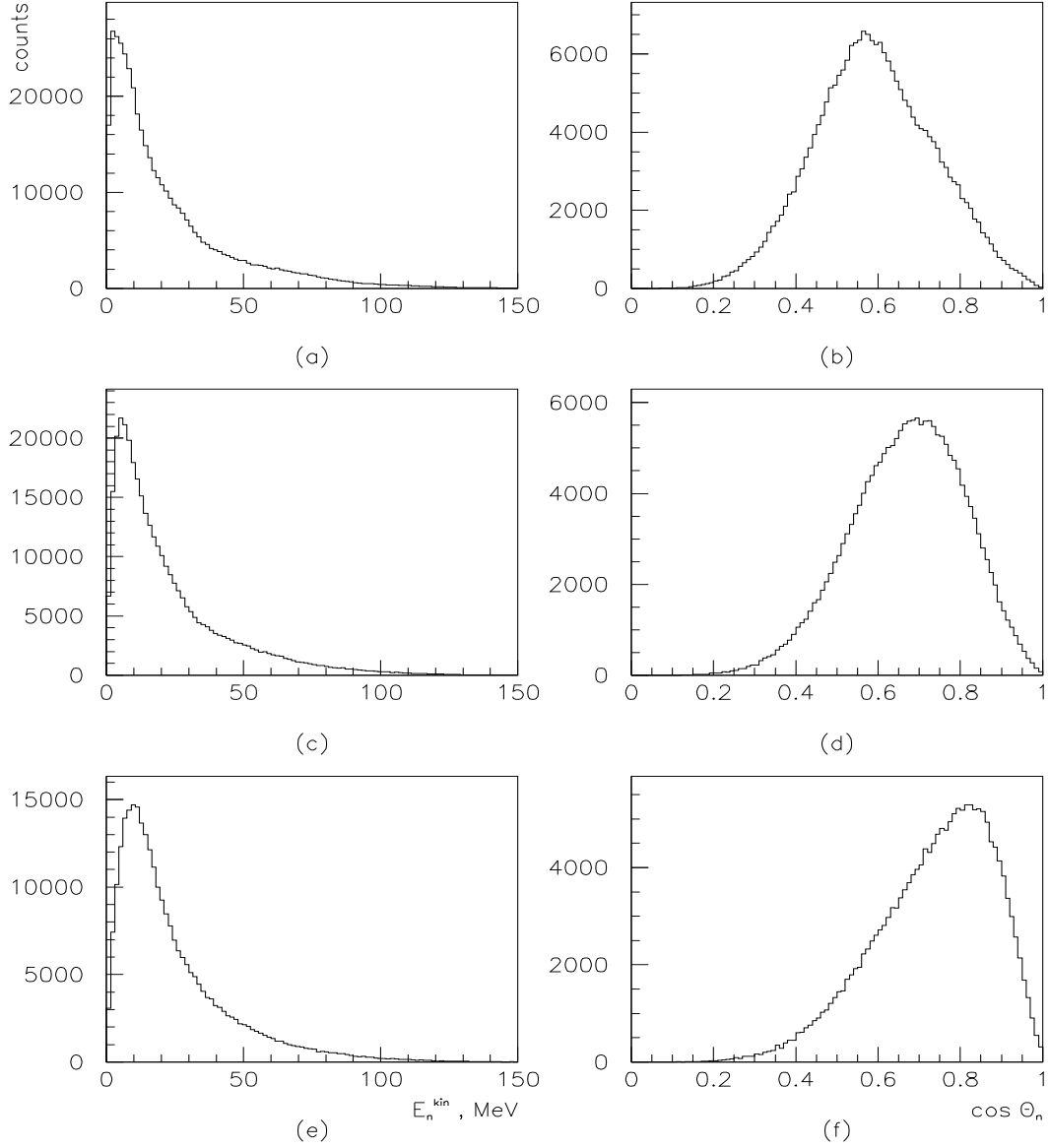


Figure 11: The energy (a,c,e) and angular (b,d,f) distributions of the nucleons from the decays of the dibaryons with different masses: (a,b) –  $M = 1900$  MeV, (c,d) –  $M = 1950$  MeV, (e,f) –  $M = 2000$  MeV.

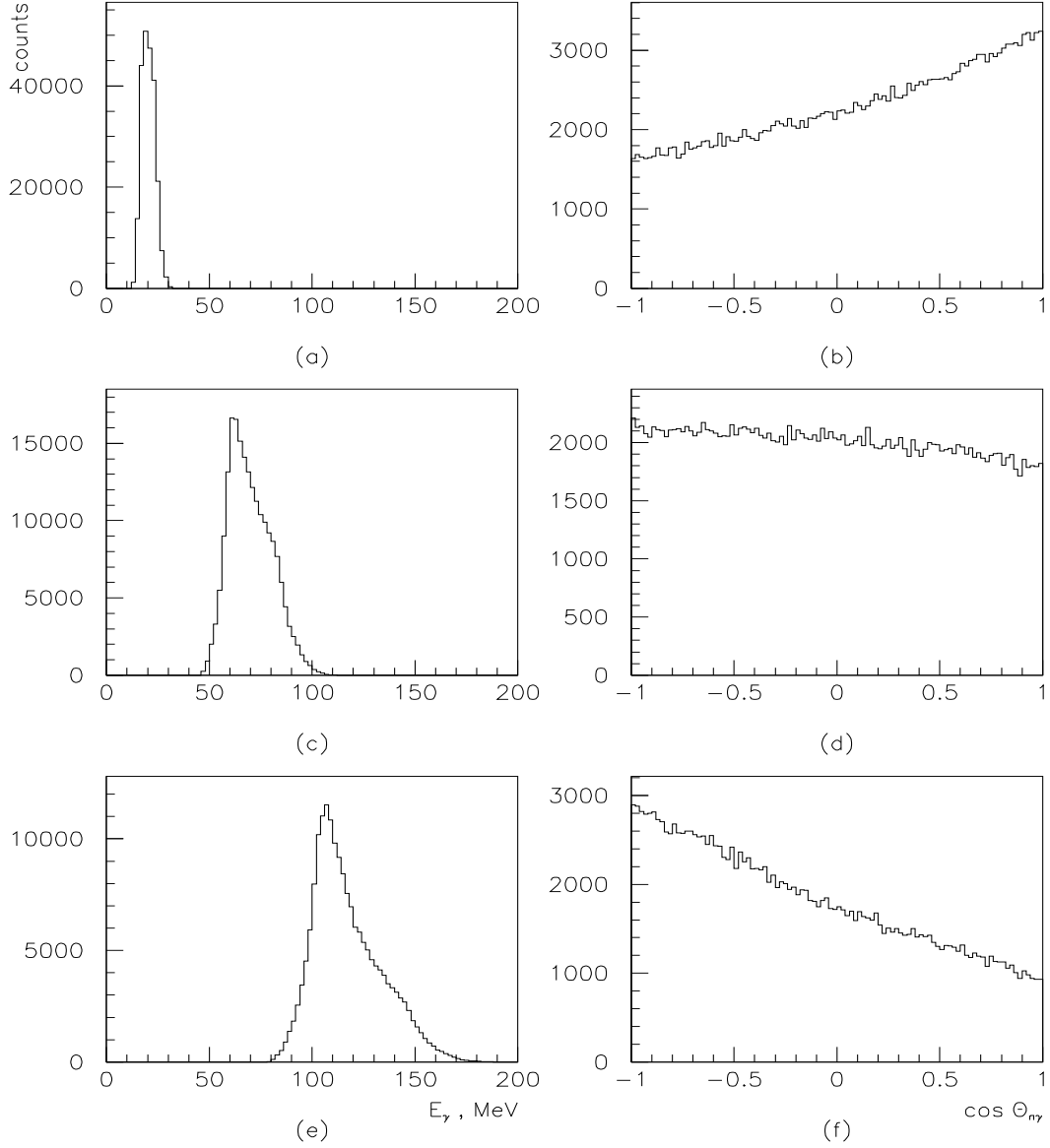


Figure 12: The energy (a,c,e) and angular (b,d,f) distributions of the photons from the decays of the SND with the different masses: (a,b) –  $M = 1900$  MeV, (c,d) –  $M = 1950$  MeV, (e,f) –  $M = 2000$  MeV.

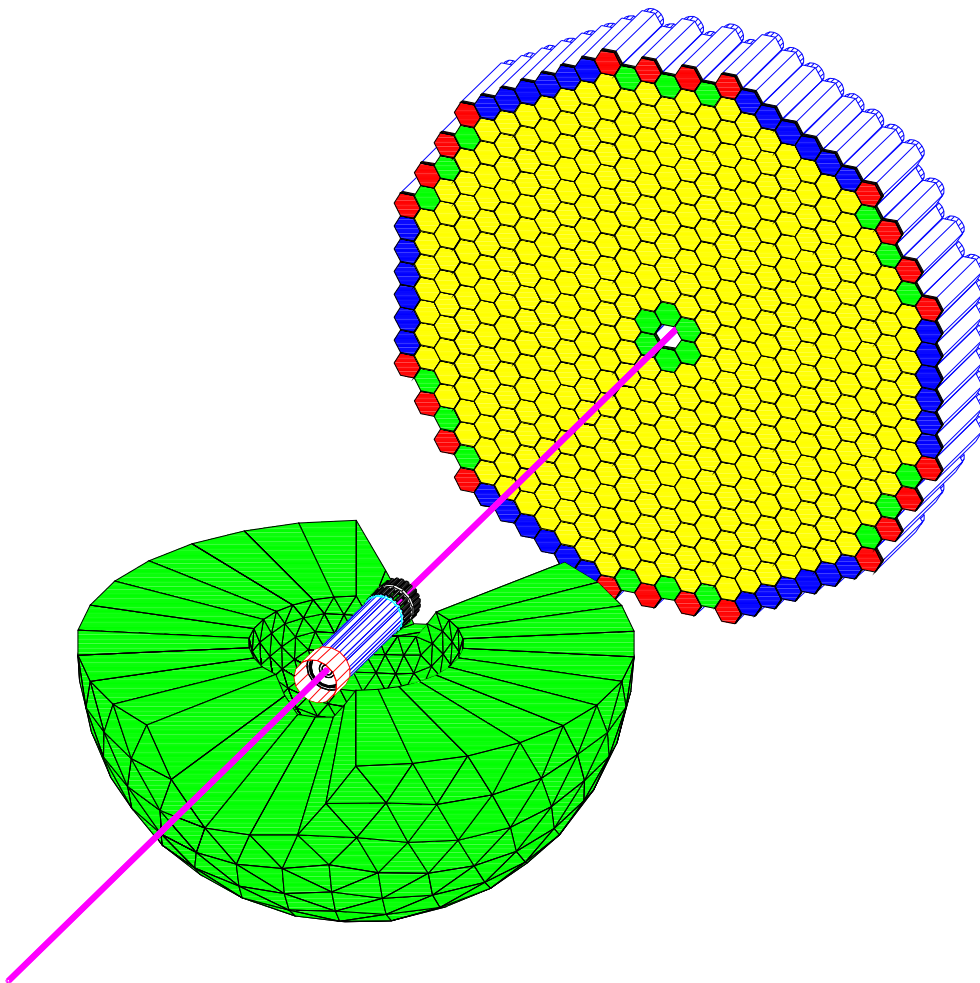


Figure 13: Crystal Ball spectrometer and TAPS

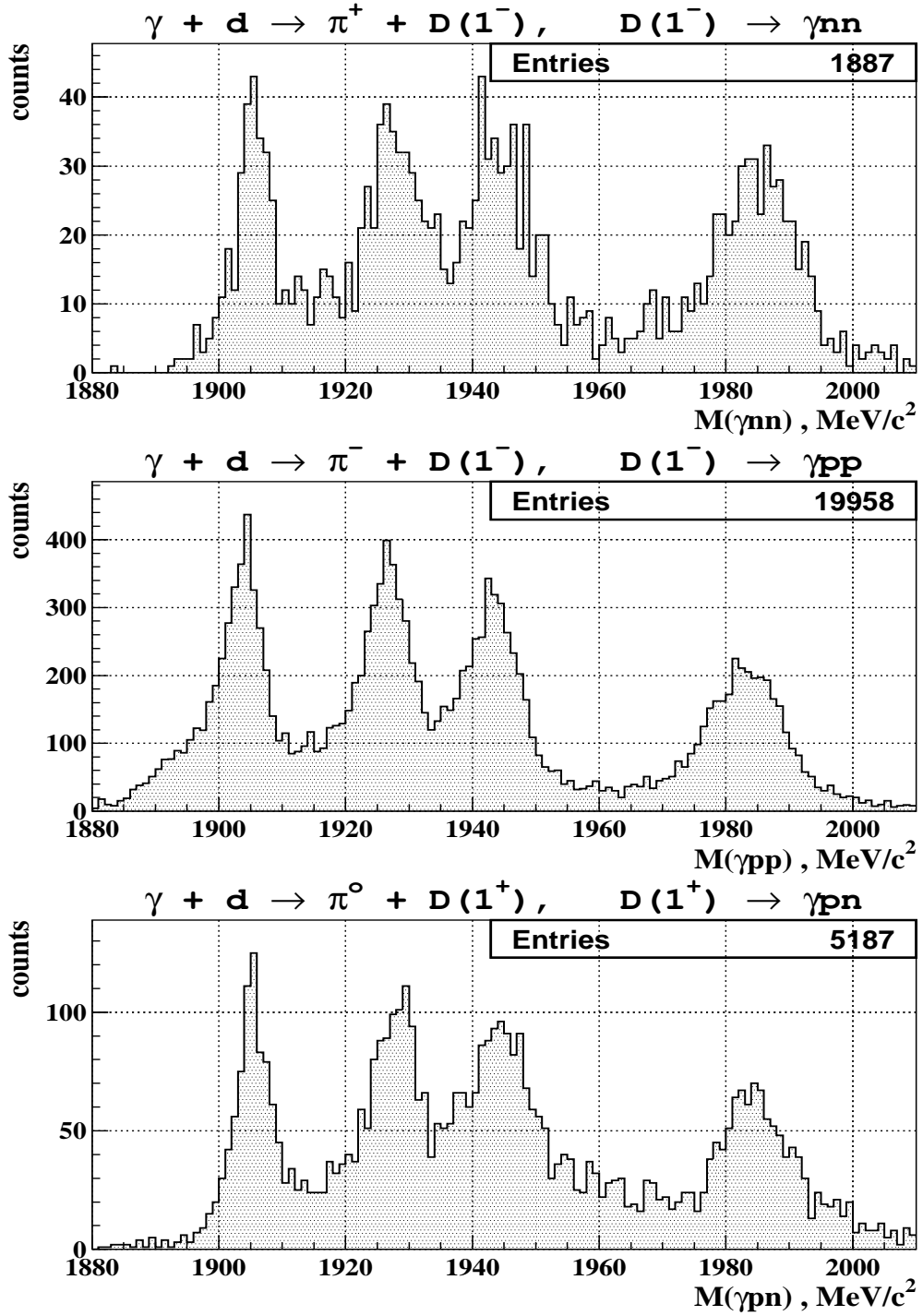


Figure 14: GEANT simulation of the SNDs with  $M = 1904, 1926, 1942,$  and  $1980 \text{ MeV}$  production in the processes  $\gamma d \rightarrow \pi^+ \gamma nn, \gamma d \rightarrow \pi^- \gamma pp,$  and  $\gamma d \rightarrow \pi^0 \gamma pn$  for 300 hours of beam time.

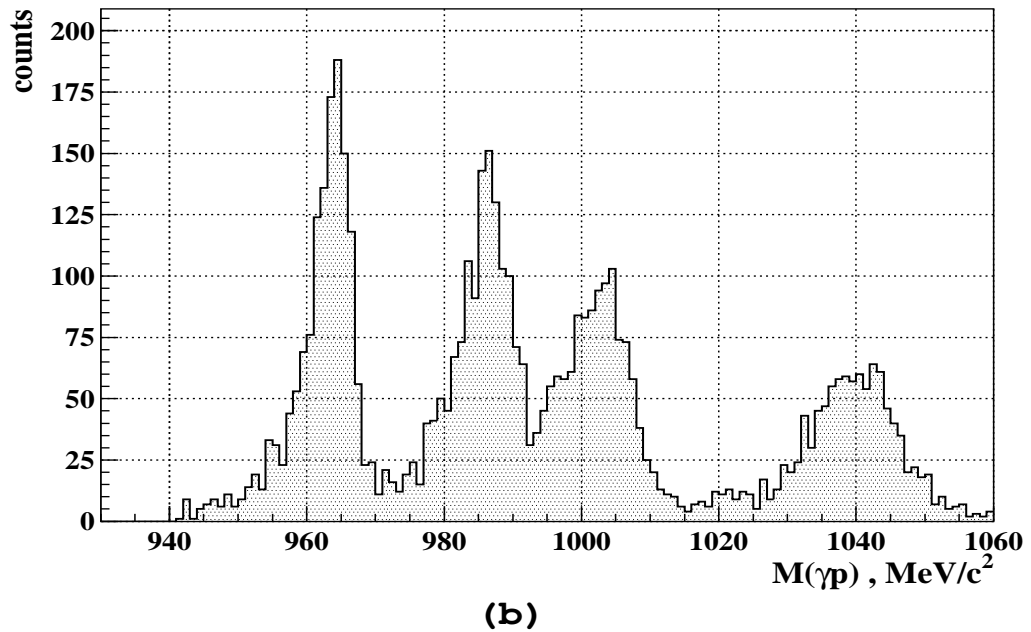
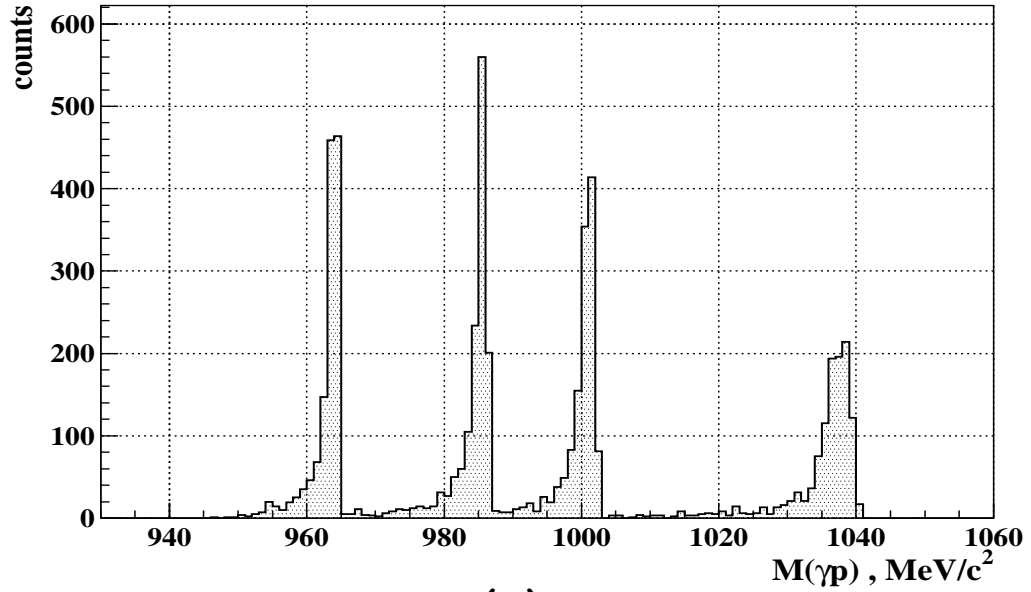
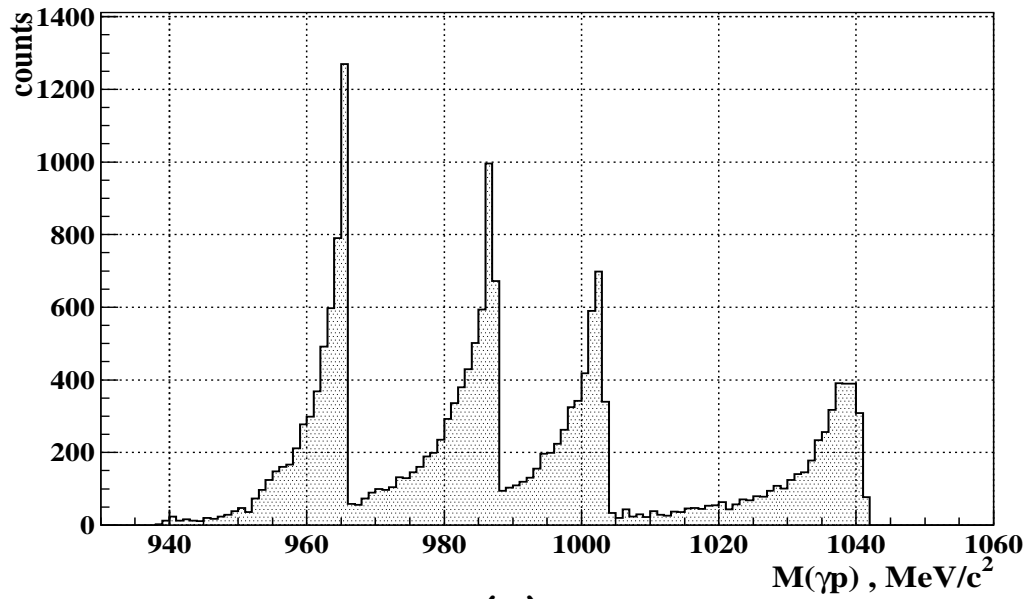
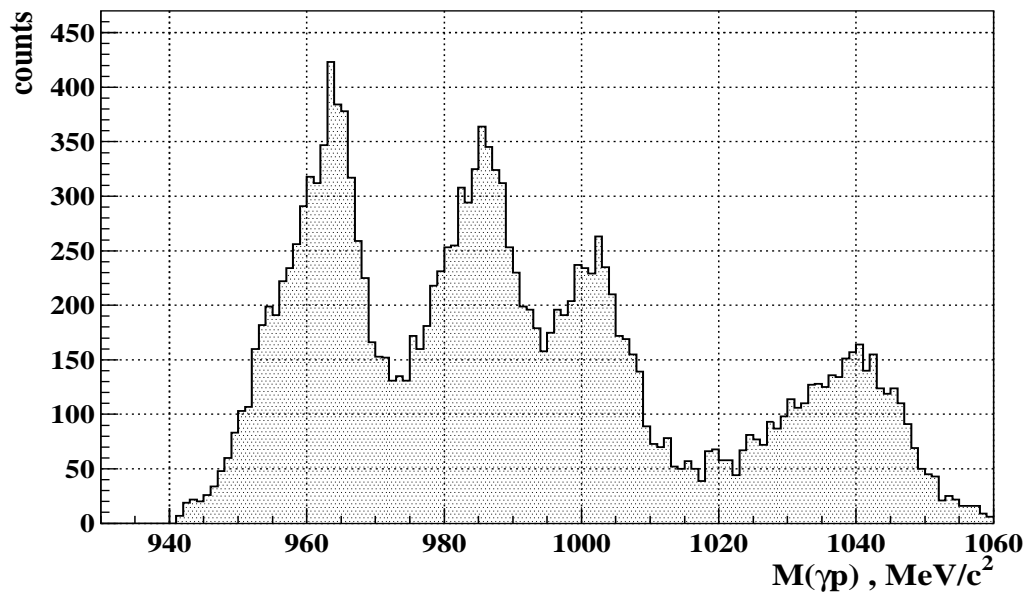


Figure 15: GEANT simulation of the invariant  $\gamma p$  and  $\gamma n$  mass spectra for the reaction  $\gamma d \rightarrow \pi^0 \gamma p n$ ; a – without an influence of the detectors; b – with an influence of the detectors



(a)



(b)

Figure 16: GEANT simulation of the invariant  $\gamma p$  mass spectra for the reaction  $\gamma d \rightarrow \pi^- \gamma pp$ ; a- without an influence of the detectors; b - with an influence of the detectors